To complete the point-to-point responses to the reviews in the author comments AC1, AC2 and AC3 and to the short comments in AC4, a marked-up version of the manuscript and the supplemental material is provided in the following.

List of relevant major changes in the manuscript:

- Change of the title of the paper to avoid the misleading phrase Euler-Lagrangian descriptor (We have replaced the phrase Euler-Lagrangian descriptor in the whole manuscript by Lagrangian descriptor M_V based on the modulus of vorticity)
- Correction of misleading statements in the introduction (pp. 2-3 in the marked up version) as well as including the references pointed out by the referees
- Extended explanation of the Lagrangian descriptors M and M_V and their features (Sect. 2 pp. 5-7 in the marked-up version)
- Change of the colorcode Fig. 1, Fig. 2, Fig. 3, Fig. 4, Fig. 5, Fig. 7, Fig. 8 and Fig. 9
- Extended explanation the idea of the eddy and eddy tracking based on M_V (p. 8 line 16 to p. 10 line 13 in the marked-up version)
- Extended discussion of the choice of τ including an improved Fig. 6 (p. 12 line 1 to p . 13 line 3 in the marked-up version)
- Partly rewritten Sect. 4.2 to clarify the concept of noise and what is aimed with the idea to add noise to the velocity field (Sect. 4.2 pp. 13-17 in the marked-up version)
- Rewritten Sect. 4.3 including a revised version of the eddy shape detection only based on M_V and an example of the eddy shapes for the western Baltic Sea instead of the seeded eddy model example (Sect. 4.3 pp. 17-22)
- New Fig. 10 showing the results of the eddy shape detection based on M_V
- New Fig. 11 showing eddy shapes for an example in the western Baltic Sea
- Rewritten Sect. 5 Discussion and conclusion explaining the advantages and disadvantages of the Lagrangian descriptor M_V and the eddy tracking based on it
- Minor changes in phrasing, grammar, spelling and punctuation in the whole manuscript as well as the correction of equation 3 (p. 5 line 20 in the marked-up version)

List of the relevant major changes in the supplemental material:

- Deleted Sect. S1 about the seeded eddy model, because we have replaced the example in the manuscript (p. 1 in the marked-up version)
- Extended Section about the algorithm of the eddy tracking. Now it includes an explanation of the eddy shape detection based on M_V and a new Fig. S3 (pp. 2-6 in the marked-up version)
- Minor changes in phrasing, grammar, spelling and punctuation in the whole supplemental material

Detecting and tracking eddies in oceanic flow fields: A ~~vorticity~~ Lagrangian descriptor based ~~Euler-Lagrangian method~~on the modulus of vorticity

Rahel Vortmeyer-Kley[1], Ulf Gräwe[2, 3], and Ulrike Feudel[1]

[1]Institute for Chemistry and Biology of the Marine Environment, Theoretical Physics/Complex Systems, Carl von Ossietzky University Oldenburg, Oldenburg, Germany
[2]Leibniz Institute for Baltic Sea Research, Rostock-Warnemünde, Germany
[3]Institute of Meteorology and Climatology, Leibniz University Hannover, Hannover, Germany

Correspondence to: Rahel Vortmeyer-Kley (rahel.vortmeyer-kley@uni-oldenburg.de)

Abstract. Since eddies play a major role in the dynamics of oceanic flows, it is of great interest to detect them and gain information about their tracks, their lifetimes and their shapes. We ~~develop a vorticity based heuristic Euler-Lagrangian descriptor utilizing the idea of Lagrangian coherent structures~~present a Lagrangian descriptor based on the modulus of vorticity to construct an eddy tracking tool. In our approach we ~~define~~ denote an eddy as a ~~region around an elliptic fixed point (eddy core) surrounded by manifolds (~~rotating region in the flow possessing an eddy ~~boundaries~~core corresponding to a local maximum of the Lagrangian descriptor and enclosed by pieces of manifolds of distinguished hyperbolic trajectories (eddy boundary). We test the performance of ~~an~~ the eddy tracking tool based on this ~~Euler-Lagrangian~~ Lagrangian descriptor using an convection flow of four eddies, a synthetic vortex street and ~~an eddy seeded model~~a velocity field of the western Baltic Sea. The results for eddy lifetime and eddy shape are compared to the results obtained with the Okubo-Weiss parameter, the modulus of vorticity and an eddy tracking tool used in oceanography. We show that the ~~Euler-Lagrangian~~ vorticity based Lagrangian descriptor estimates lifetimes closer to the analytical results than any other method. Furthermore we demonstrate that eddy tracking based on this descriptor is robust with respect to certain types of noise which makes it a suitable ~~tool~~ method for eddy detection in velocity fields obtained from observation.

1 Introduction

Transport of particles and chemical substances mediated by hydrodynamic flows are important components in the dynamics of ocean and atmosphere. For this reason, there is an increasing interest in identifying particular structures in the flows such as eddies or transport barriers to understand their role in transport and mixing of the fluid as well as their impact on ~~e.g. marine biology~~ marine biology for instance. Of particular interest in oceanography are eddies, which can be responsible for the confinement of plankton within them and hence, important for the development of plankton blooms (Abraham (1998); Martin et al. (2002); Sandulescu et al. (2007)). Such eddies possess a large variety of sizes and lifetimes. To tackle the problem of recognizing such eddies in aperiodic flows, different approaches have been developed: on the one hand, there are several methods available which are inspired by dynamical systems theory (~~Haller (2015)~~Haller (2015); Mancho et al. (2013) and references

therein), on the other hand, numerical software for automated eddy detection has been developed in oceanography based on either physical quantities of the flow (~~Okubo (1970); Weiss (1991)~~Okubo (1970); Weiss (1991); Nencioli et al. (2010)) or geometric measures (Sadarjoen and Post (2000)).

Algorithms for finding eddies in fluid flows are applied in very different fields of science such as in atmospheric science (Koh and Legras (2002)), celestial mechanics (Gawlik et al. (2009)), biological oceanography (Bastine and Feudel (2010); Huhn et al. (2012)) and the dynamics of swimmers (Wilson et al. (2009)). The largest field of application is oceanography, since oceanic flows contain a large number of mesoscale eddies of size 100-200 km, which are important components of advective transport. Their emergence and lifetime influences the transport of pollutants (Mezić et al. (2010); Olascoaga and Haller (2012); Tang and Luna (2013)) or plankton blooms (Bracco et al. (2000); Sandulescu et al. (2007); Rossi et al. (2008); Hernández-Carrasco et al. (2014)). There is an increasing number of eddy resolving data sets available provided either by observations (Donlon et al. (2012)) or by numerical simulations (Thacker et al. (2004); Dong et al. (2009)). Subsequently there is a growing interest in the census of eddies, their size and lifetimes depending on the season. This task requires robust algorithms for the computation of eddy boundaries as well as the precise detection of their appearance and disappearance in time based on numerical velocity fields (Petersen et al. (2013); Wischgoll and Scheuermann (2001); Dong et al. (2014)) as well as altimetry data (Chaigneau et al. (2008); Chelton et al. (2011)). However, the huge amount of available data poses a challenge to data analysis. As pointed out in Chaigneau et al. (2008) mesoscale and submesoscale eddies cannot be extracted from a turbulent flow without a suitable definition and a competitive automatic identification algorithm. Several such algorithms have been developed based on the various concepts mentioned above. In the following we will briefly discuss several of those algorithms.

Based on dynamical systems theory, one can search for Lagrangian coherent structures (LCS) which describe the most repelling or attracting manifolds in a flow (Haller and Yuan (2000)). The time evolution of these invariant manifolds make up the Lagrangian skeleton for the transport of particles in fluid flows. LCS can be considered as the organizing centres of hydrodynamic flows. Their computation is based on the search for stationary curves of shear in case of hyperbolic or parabolic LCS. Elliptic LCS like eddies are computed as stationary curves of averaged strain (Haller and Beron-Vera (2013); Karrasch et al. (2015); Onu et al. (2015)) or Lagrangian-averaged vorticity deviation (Haller et al. (2016)). Other methods to determine whether an eddy can be identified in the flow employ average Lagrangian velocities (Mezić et al. (2010)) or burning invariant manifolds (Mitchell and Mahoney (2012)). The latter have been introduced originally to track fronts in reaction diffusion systems (Mahoney et al. (2012)) but have been recently extended to the detection of eddies (Mahoney and Mitchell (2015)). A completely different approach which connects geometric properties of a flow with probabilistic measures utilizes transfer operators to identify LCS (Froyland and Padberg (2009)). Another ~~, more heuristic~~ approach is the computation of distinguished hyperbolic trajectories (DHT) and their stable and unstable manifolds to identify Lagrangian coherent structures in a flow. DHTs can be considered as a generalization of stagnation points of saddle type and their separatrices to general time-dependent flows (Ide et al. (2002); Wiggins (2005); Mancho et al. (2006)). ~~Algorithms to compute~~ DHTs and their manifolds ~~rely on the computation of the ridges of Lagrangian descriptorssuch as e.g. arc lengths along trajectories of particles in the flow~~ can be computed using Lagrangian descriptors, which integrate intrinsic physical properties for a finite time and thereby reveal the geometric structures in phase space (Mancho et al. (2013)). Stable and unstable manifolds can also be calculated using the ridges of finite time or

finite size Lyapunov exponents (FTLE or FSLE) (~~Artale et al. (1997); Boffetta et al. (2001); d'Ovidio et al. (2004)~~ Artale et al. (1997); Boffetta et al. (2001); d'Ovidio et al. (2004); Branicki and Wiggins (2010)) using the idea that initially nearby particles in a flow will move apart in stretching regions while they will move closer to each other in contracting regions.~~The unstable manifolds are often called material lines in 2d (Koh and Legras (2002)) and surfaces in 3d flows (Haller (2001); Bettencourt et al. (2012); Froyland et al. (2012)), since particles would gather along these manifolds identifying them as barriers to transport. While most of the algorithms mentioned above possess the property of objectivity , i.e. they are invariant with respect to certain transformations of the Eulerian coordinate system, the method of Lagrangian descriptors lacks this property (Haller (2015)). Nevertheless, they are often used since the implementation of this method is easy and the computation is fast. This is particularly important when analysing large velocity fields with lots of LCS appearing and disappearing. Hence, the heuristic~~

Despite the discussion about objectivity (cf. Haller's short comment SC2 in the discussion of this paper, Mancho's editor comment EC1 and Mendoza and Mancho (2012)) the method of Lagrangian descriptors is very appealing and ~~might be more~~ is appropriate to gain insight into oceanographic flows~~in a considerable amount of time~~. It has already been successfully applied to compute Lagrangian coherent structures in the Kuroshio current (~~Mendoza et al. (2010); Mendoza and Mancho (2010))and~~ Mendoza et al. (2010); Mendoza and Mancho (2010, 2012)), in the Polar Vortex (de la Cámara et al. (2012)), in the North-Western Mediterranean Sea (Branicki et al. (2011)) as well as analysing the possible dispersion of debris from the Malaysian Airlines flight MH370 airplane in the Indian Ocean (García-Garrido et al. (2015)).

In the recent years there has been some effort to derive Eulerian quantities which can be used to draw conclusions about Lagrangian transport phenomena (Sturman and Wiggins (2009); McIlhany et al. (2011); McIlhany and Wiggins (2012); McIlhany et al. (2015)).

In oceanography, one of the most popular methods to identify eddies is based on the Okubo-Weiss parameter (Okubo (1970); Weiss (1991)). This method relies on the strain and vorticity of the velocity field, and has been applied to both, numerical ocean model output and satellite data (Isern-Fontanet et al. (2006); Chelton et al. (2011)). Often, the underlying velocity field is derived from altimetric data under the assumption of geostrophic theory. In this approach two limitations can appear. First, the derivation of the velocity field can induce noise in the strain and vorticity field. This is usually reduced by applying a smoothing algorithm, which might, in turn, remove physical information. Secondly, Douglass and Richman (2015) show that eddies can have a significant ageostrophic contribution. Thus, the detection might fail when relying on geostrophic theory. A slightly different approach was developed by Yang et al. (2001) and Fernandes et al. (2011), who used the signature of eddies in the sea surface temperature (SST) to detect them. ~~Anyhow, the~~ The partially sparse coverage of satellite SST data limits the application of this method.

Sadarjoen and Post (2000) developed a tracking algorithm that is based on the flow geometry. The assumption is that eddies can be defined as features characterized by circular or spiral streamlines around the core of an eddy. The streamlines are derived from the velocity field. Additionally, the change of direction of the segments that compose the streamline (winding angle) is computed for each streamline. Chaigneau et al. (2008) applied this winding angle approach to a data set of the South Pacific. Moreover, they compared the winding angel method to the Okubo-Weiss approach and concluded that the former is more

successful in detecting eddies and more important with a much smaller excess of detection errors. A further method based on geometric properties is proposed by Nencioli et al. (2010). The underlying idea is that within an eddy, the velocity field changes its direction in a unique way. Moreover, the relative velocity in the eddy core should vanish and should be enclosed by closed stream lines. This detection and tracking algorithm was successfully applied by Dong et al. (2012) in the Southern California Bight. In addition, the detection algorithm of Nencioli et al. (2010) has the advantage that its application is not limited to surface fields (Isern-Fontanet et al. (2006); Chelton et al. (2011); Fernandes et al. (2011)). Thus, it is possible to track eddies in the interior of the ocean, without any surface signature.

In this paper we develop an eddy detection and tracking tool based on the ~~heuristic~~ method of the Lagrangian descriptor introduced by Mancho and co-workers (Madrid and Mancho (2009); Mancho et al. (2013)). ~~Instead of using the arc length of trajectories~~ For the purpose of automated eddy detection we propose to use the modulus of the vorticity as the scalar quantity to be computed along a trajectory ~~. We find this method combining the Eulerian and Lagrangian approaches to be more reliable in the detection of eddies and their lifetimes than other methods. More specifically we~~ instead of using the arc length of trajectories. We compare our method to four others, namely the original Lagrangian descriptor using the arc length (Madrid and Mancho (2009); Mendoza et al. (2010)), an oceanographic method based on geometric properties of the flow field (Nencioli et al. (2010)) and detection tools which employ the Okubo-Weiss parameter (Okubo (1970); Weiss (1991)) and the vorticity itself.

The paper is organized as follows: Sect. 2 briefly reviews the Eulerian concepts vorticity and Okubo-Weiss parameter, the Lagrangian ~~descriptor~~ descriptors M based on the arc length and ~~introduces our Euler-Lagrangian descriptor. To demonstrate~~ M_V based on the modulus of vorticity. To compare the performance of ~~this method compared to the Lagrangian descriptor~~ the two Lagrangian descriptors and the Eulerian concepts we use two simple velocity fields: the model of four counter rotating eddies and a modified van ~~Karman~~ Kármán vortex street in Sect. 3. In Sect. 4 we describe the implementation of the ~~Euler-Lagrangian descriptor~~ Lagrangian descriptor based on the modulus of vorticity as a tracking tool identifying eddy lifetimes (Sect. 4.1) and compare the results again with the aforementioned other methods. In Sect. 4.2 we study the performance of the method in cases where we corroborate the velocity fields with noise to test the robustness of the method if applied to velocity fields obtained from observational data. Finally in Sect. 4.3 we compare the Eulerian and the ~~Euler-Lagrangian~~ Lagrangian view of the eddy shape with application to the modified van ~~Karman~~ Kármán vortex street and to a velocity field ~~which is similar to the one introduced by Abraham (1998) to study the impact of mesoscale hydrodynamic structures on plankton blooms~~from oceanography describing the dynamics of the Western Baltic Sea (Gräwe et al. (2015a)). We conclude the paper with a discussion in Sect.5.

2 From Eulerian ~~and~~ to Lagrangian methods~~to an Euler-Lagrangian method~~

The dynamics of a fluid can be characterized employing two different concepts: the Eulerian and the Lagrangian view. While the Eulerian view uses quantities describing different properties of the velocity field, the Lagrangian view provides quantities from the perspective of a moving fluid particle. Out of the variety of different Eulerian and Lagrangian methods mentioned

in the introduction, we recall here briefly only those concepts, which will be important for our development of a measure to identify eddies in a flow.

An Eulerian method to describe the circulation density of a velocity field in hydrodynamics is vorticity $\boldsymbol{W}(\boldsymbol{x},t)$ defined as the curl of the velocity field $\boldsymbol{v}(\boldsymbol{x},t)$.The vorticity associates a vector to each point in the fluid representing the local axis of rotation of a fluid particle. It displays areas with a large circulation density like eddies as regions of large vorticity and eddy cores as local maxima.

Another Eulerian quantity is the Okubo-Weiss parameter OW. It weights the strain properties of the flow against the vorticity properties and distinguishes so strain dominated areas from vorticity dominated one. The Okubo-Weiss parameter is defined as

$$OW = s_n^2 + s_s^2 - \omega^2, \tag{1}$$

where the normal strain component s_n, the shear strain component s_s and the relative vorticity ω of a two dimensional velocity field $\boldsymbol{v} = (u, v)$ are defined as

$$s_n = \frac{\partial u}{\partial x} - \frac{\partial v}{\partial y}, \quad s_s = \frac{\partial v}{\partial x} + \frac{\partial u}{\partial y} \quad \text{and} \quad \omega = \frac{\partial v}{\partial x} - \frac{\partial u}{\partial y}. \tag{2}$$

Eddies are areas having a negative Okubo-Weiss parameter with a local minimum at the eddy core because here the vorticity component outweighs the strain component, while strain dominated areas are characterized by a positive Okubo-Weiss parameter.

A Lagrangian view on the dynamics of the velocity field is given by the Lagrangian descriptor developed by Mancho and coworkers (Madrid and Mancho (2009)). A more general definition of the Lagrangian descriptor is outlined in Mancho et al. (2013). Here we ~~use~~ focus on the Lagrangian descriptor based on the arc length of a trajectory~~. It is defined as~~ , defined as

$$M(\boldsymbol{x}^*, t^*)_{\boldsymbol{v},\tau} = \int_{t^*-\tau}^{t^*+\tau} \sqrt{\sum_{i=1}^{n} \left(\frac{dx_i(t)}{dt}\right)} \left(\sum_{i=1}^{n} \left(\frac{dx_i(t)}{dt}\right)^2\right)^{1/2} dt \tag{3}$$

with $\boldsymbol{x}(t) = (x_1(t), x_2(t)...x_n(t))$ being the trajectory of a fluid particle in the velocity field $\boldsymbol{v}$ that is defined in the time interval $[t^* - \tau,\ t^* + \tau]$ and going through the point $\boldsymbol{x}^*$ at time t^*.

The Lagrangian descriptor M ~~can distinguish stable and unstable manifolds as well as hyperbolic and elliptic regions in the velocity field at the same time~~ yields singular features that can be interpreted as time-dependent "phase space structures" like (time-dependent or moving) elliptic or hyperbolic "fixed" points (denoted as distinguished elliptic or hyperbolic trajectories DET and DHT respectively in Madrid and Mancho (2009)) and their time dependent stable and unstable manifolds (Mancho et al. (2013); Wiggins and Mancho (2014)). The reason ~~is~~ for the singular features of M is, that M accumulates different values of the arc length depending on the dynamics in the region. Trajectories that have a similar dynamical evolution ~~,~~ yield similar values of M. When the dynamics changes abruptly, M will change too. This is the case at ~~fixed points and~~ distinguished hyperbolic trajectories (DHTs) and their stable and unstable manifolds. ~~In case of manifolds trajectories~~ Trajectories on both sides of the manifold have a different behaviour compared to the behaviour of the trajectories on the

manifold. Either they approach the manifold very fast or ~~the~~ they move away from the manifold very fast. In both cases they accumulate ~~a~~ larger values of M in a given time interval than trajectories on the manifold. Therefore~~the manifold is displayed as a~~ , the singular line of M in a ~~contour~~ color-coded plot of M ~~. Fixed points themselves correspond to local minima~~ can be interpreted as corresponding to a manifold. If a trajectory stays in a region or at one point it accumulates a small or zero value of M ~~. Here the trajectories do not leave the region of~~ and M becomes a local minimum. While DHTs have been extensively studied, distinguished trajectories possessing an elliptic type are less understood. However, such trajectories can also be identified as singular features of M being surrounded by an elliptic region in the sense of Mancho et al. (2013). For an extensive discussion about the notion of hyperbolic and elliptic regions in flows we refer to Mancho et al. (2013).

For each instant of time t^* the ~~fixed point and accumulate small values of~~ color-coded plots of M ~~. As a consequence the Lagrangian descriptor~~ can be interpreted as a "snapshot" of the phase space, where the minima correspond to one point of a DHT or a distinguished trajectory surrounded by an elliptic region. When t^* is changing M ~~cannot distinguish between elliptic and hyperbolic fixed pointsand is therefore not suitable to identify eddies without using a second criterion. Therefore the Eulerian and the Lagrangian view on the dynamics in a flow will be combined into a new quantity.~~ reveals the time evolution of the phase space and loosely speaking distinguished hyperbolic trajectories can be considered as "moving saddle points", distinguished trajectories surrounded by an elliptic region in the sense of Mancho et al. (2013) as "moving elliptic points". Due to the arbitrary time-dependence of the flow, both, the DHTs and the distinguished trajectories surrounded by an elliptic region are time-dependent and exist in general only for a finite time in a time-dependent flow. Hyperbolicity in case of DHT refers to the fact that along those trajectories Lyapunov exponents are positive or negative, but not zero except for the direction along the trajectory (Mancho et al. (2013)).

~~As already~~ Because the Lagrangian descriptor M would display minima in both cases, i.e. DHT and distinguished trajectories surrounded by an elliptic region, a second criterion is needed to distinguish them properly. To avoid such additional distinction criterion, we suggest a Lagrangian descriptor based on the modulus of vorticity to simplify the automated eddy detection. We emphasize, that it has already been pointed out by Mancho et al. (2013) that any intrinsic physical or geometrical property of trajectories can be used to construct a Lagrangian descriptor by integrating this property along trajectories over a certain time interval. Therefore, we introduce a vorticity based Lagrangian descriptor M_V in which the physical quantity is the modulus of the vorticity W of a velocity field $\boldsymbol{v}(\boldsymbol{x},t)$

$$W(\boldsymbol{x},t) = |\nabla \times \boldsymbol{v}(\boldsymbol{x},t)|\,. \tag{4}$$

We define the ~~Euler-Lagrangian~~ Lagrangian descriptor M_V ~~as~~ based on the modulus of vorticity as

$$M_V(\boldsymbol{x}^*,t^*)_\tau = \int_{t^*-\tau}^{t^*+\tau} (W(\boldsymbol{x},t))^{\gamma}{}^{1/2} dt. \tag{5}$$

~~with $\gamma = \frac{1}{2}$. The Euler-Lagrangian~~ The Lagrangian descriptor M_V ~~combines the Eulerian and the Lagrangian view of a dynamical system by measuring~~ based on the modulus of vorticity measures the Eulerian quantity modulus of vorticity along a trajectory (Lagrangian view) passing through a position $\boldsymbol{x}^*$ at time t^* in a time interval $[t^*-\tau,\ t^*+\tau]$. Within this time

interval trajectories accumulate different values of M_V. As the arc length based Lagrangian descriptor M, the Lagrangian descriptor M_V based on the modulus of vorticity displays singular features as lines or local minima or maxima. In case of ~~elliptic fixed points, the~~ local maxima, a trajectory does not leave the ~~eddy core but collects~~ region of large values of modulus of vorticity~~within this region. Hence, elliptic fixed points are local maxima in the contour plot of M_V~~. Such regions are typical for the inner part of an eddy. Therefore, a local maximum corresponds to the eddy core and can be interpreted as a "snapshot" of the distinguished trajectory at time t^* surrounded by an elliptic region in the sense of Mancho et al. (2013). By contrast, ~~hyperbolic fixed points are local minima . Here the trajectories stay~~ local minima of M_V arise if a trajectory stays in a region of small values of modulus of vorticity~~values. The manifolds are lines along which strain dominates and therefore the collected modulus of vorticity along a trajectory is smaller than in~~ . In analogy with the singular lines in case of M, singular lines of M_V can be interpreted as the boundaries of regions of different dynamical behaviour. ~~The~~ In this sense they can be understood as manifolds of the DHTs.

The local maxima and the singular lines of M_V will be used to construct an eddy tracking tool based on the following concept of an eddy: We denote an eddy as being bounded by pieces of stable and unstable manifolds ~~are again lines of small~~ of DHTs (according to Branicki et al. (2011) and Mendoza and Mancho (2012)) surrounding an area in which the flow is rotating. The manifolds correspond to singular lines in M_V which are used to describe the eddy boundaries. The eddy core is considered to be a local maximum of M_V within this bounded region and can be interpreted as one point of a distinguished trajectory surrounded by an elliptic region.

In case of M_V as well as in case of M the resolution of ~~structures like manifolds and fixed points~~ these structures depends on the choice of the parameter τ that gives the length of the time interval. Structures that live shorter than 2τ cannot be resolved. Even structures that live longer than 2τ can only be resolved if τ is chosen large enough. The choice of τ depends on the structure and the time scale of the flow field considered. Within the range of the time scale of the problem that should be resolved some variation of τ is needed until the optimal τ for a given problem is found.

3 Eddies in a flow: Comparing ~~the~~ Eulerian ~~, Lagrangian~~ and ~~Euler-Lagrangian~~ Lagrangian methods

To compare the performance of the proposed ~~Euler-Lagrangian method to others~~ Lagrangian descriptor based on the modulus of vorticity to the others, two test cases ~~, namely -~~ a convection flow consisting of four counter rotating eddies and a model of a vortex street ~~, -~~ are used. The four counter rotating eddies are ~~used~~ employed to show that different methods detect different aspects of the eddies. Additionally, we discuss how the displayed structure depends on the chosen τ. The vortex street is particularly used to test how suitable our method is to detect and track eddies in comparison to other methods and how well they all estimate eddy lifetimes and shapes. This way we gain insight into performance, advantages and disadvantages of the proposed method compared to the others.

To give a complete view of the advantages and disadvantages the results of the different test cases are interpreted in a coherent discussion after presenting all results.

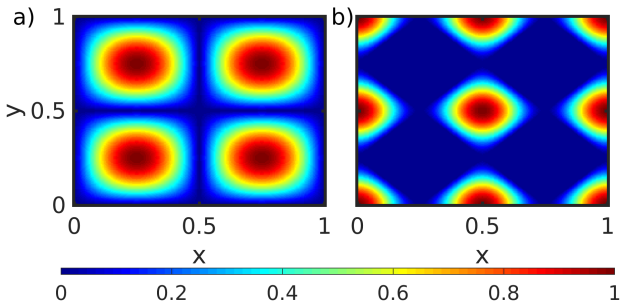

Figure 1. Colour-coded representation of the modulus of vorticity (a), Okubo-Weiss-Parameter (b) for the eddy field in Eq. (6). All plots are normalized to the maximum value.

The ~~equation~~ equations of motion of fluid particles in a convection flow of four counter rotating eddies are given by

$$u = \dot{x} = \sin(2\pi \cdot x) \cdot \cos(2\pi \cdot y) \quad \text{and} \quad v = \dot{y} = -\cos(2\pi \cdot x) \cdot \sin(2\pi \cdot y). \tag{6}$$

We compute the four different quantities, modulus of vorticity, Okubo-Weiss parameter, ~~Lagrangian descriptor and Euler-Lagrangian descriptor~~ the two Lagrangian descriptors M and M_V on a spatial domain ~~$(0,\,1) \times (0,\,1)$~~ $[0,\,1] \times [0,\,1]$. To this end, the spatial domain is decomposed into a discrete grid (201×201) and the different methods are calculated for each grid point. The results are presented in Figs. 1 and 2.

The model of the vortex street consists of two eddies that emerge at two given positions in space, travel a distance L in positive x-direction and fade out. The two eddies are counter rotating. They emerge and die out periodically with a time shift of half a period. The model is adapted from Jung et al. (1993) and Sandulescu et al. (2006) with the difference that the cylinder as the cause of eddy formation and its impact on the flow field due to its shade is neglected. In this sense, the eddies emerge non-physically out of ~~the blue~~ nowhere, but all quantities like lifetime and radius to be estimated by means of eddy tracking are then given analytically and make up a perfect test scenario. A detailed description of the model can be found in the supplemental material to this article. Again all methods are applied to this velocity field using a (302×122) grid. Unless otherwise stated, the time interval τ for the Lagrangian ~~and Euler-Lagrangian~~ methods is set to 0.15 times the lifetime of an eddy. The results are presented in Fig. 3.

These two test cases reveal the following characteristics of the properties of coherent structures in a flow: Eulerian ~~, Lagrangian~~ as well as ~~Euler-Lagrangian methods identify eddy cores (moving elliptic fixed points)~~ Lagrangian methods display eddy cores as local maxima (modulus of vorticity, M_V) or local minima (Okubo-Weiss, M) of the respective quantity (Fig.1,2,3). ~~The Lagrangian and the Euler-Lagrangian method identify moving hyperbolic fixed points as local minima~~ Local minima of the Lagrangian methods correspond to DHTs (Fig. 2e, f). For the Lagrangian descriptor M the ~~centre~~ core of the eddy as well as the ~~moving hyperbolic fixed point~~ DHT are indistinguishable since they are both displayed as local minima of M. ~~Our Euler-Lagrangian~~ The Lagrangian descriptor M_V based on modulus of vorticity can clearly distinguish between the ~~centres~~ core of an eddy and ~~moving hyperbolic points~~ a DHT (Fig. 2a-c). For this reason~~Eulerian and Euler-Lagrangian methods ,~~

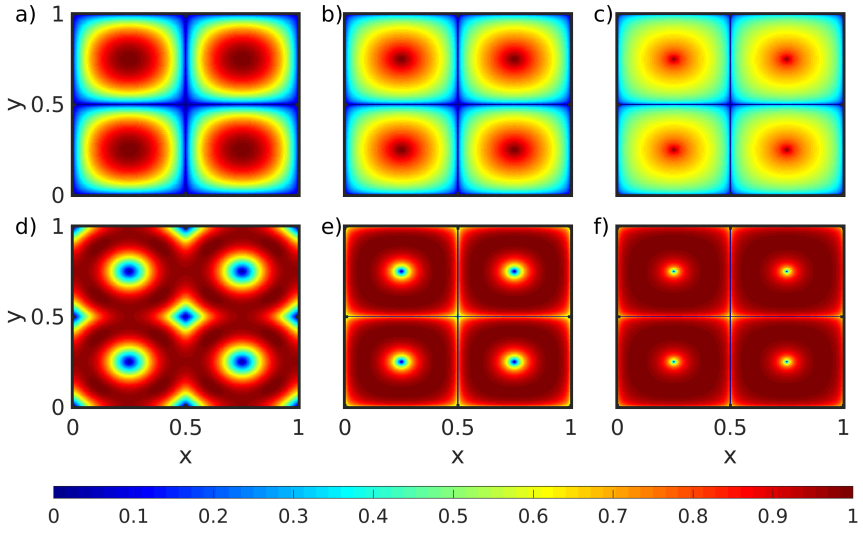

Figure 2. Colour-coded representation of the ~~Euler-Lagrangian~~ Lagrangian descriptor M_V (a-c) and the Lagrangian descriptor M (d-f) for the eddy field in Eq. (6) with τ chosen as 0.5 (a and d), 25 (b and e) and 100 (c and f). All plots are normalized to the maximum value.

Eulerian methods and the Lagrangian descriptor M_V are more appropriate than the Lagrangian descriptor M for ~~identifying eddiesin a general time-dependent velocity field~~an automated identification of eddies, since no further criteria are needed.

To characterize Lagrangian coherent structures in a flow not only ~~elliptic fixed points~~ distinguished trajectories surrounded by an elliptic region in the sense of Mancho et al. (2013) associated with eddy cores and ~~moving hyperbolic fixed points~~ DHTs have to be identified but also the stable and unstable manifolds associated with the latter to find eddy boundaries ~~.~~ according to the concept of an eddy in Sect. 2. Those manifolds are ~~only identifiable~~ visible as singular lines in the ~~contour plot using~~ color-coded plot of the Lagrangian descriptor M (Fig. 2 d-f, 3 c) and the ~~Euler-Lagrangian~~ Lagrangian descriptor M_V (Fig. 2 a-c, 3 d) respectively.

How detailed the displayed fine structure of the Lagrangian ~~descriptor~~ descriptors M and ~~the Euler-Lagrangian descriptor~~ M_V is represented depends on the chosen value of the time interval τ. It ranges from no clear structure for small τ (Fig. 2 a and d) to a detailed structure for large τ (Fig. 2 c and f).

From these properties, distinction ~~elliptic and hyperbolic fixed points~~ between DHTs and eddy cores and identification of manifolds, we can conclude that the ~~Euler-Lagrangian~~ Lagrangian descriptor M_V is ~~the most suitable quantity to compute when studying oceanographic flows with respect to~~ a suitable method for an automated search for eddies ~~. It is the only quantity~~ in oceanographic flows. Out of the four ~~quantities considered which~~ considered quantities M_V allows for a clear identification of eddy cores and the stable and unstable manifolds of ~~hyperbolic fixed points which can be used~~ DHTs necessary to get more insight into the size of eddies with the least number of check criteria. For this reason we suggest to use M_V as the basis for an

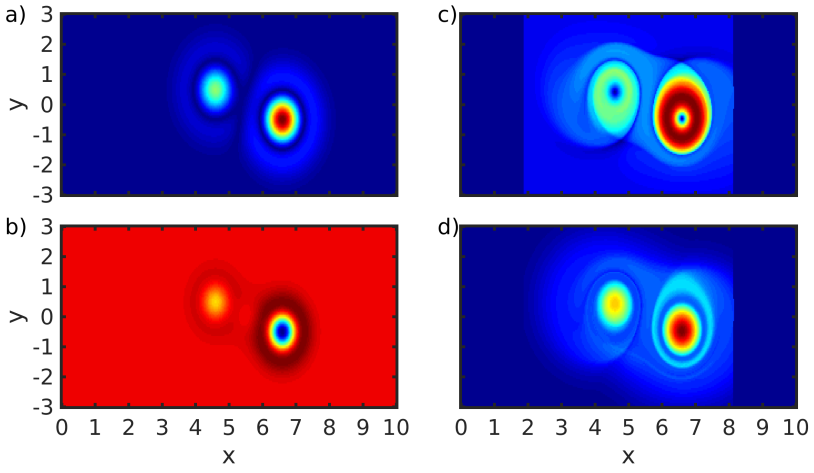

Figure 3. Modulus of vorticity (a), Okubo-Weiss parameter (b), Lagrangian descriptor M (c) and ~~Euler-Lagrangian~~ Lagrangian descriptor M_V (d) for the ~~hydrodynamical~~ hydrodynamic model of a vortex street at $t = 0.151$ with $\tau = 0.15$, normalized to the maximum value. Blue colours indicate small values yellow large values of the depicted quantity. The dark blue regions in (c) and (d) are regions where the trajectories have left the region of interest.

eddy tracking tool. How these properties of M_V are implemented into an eddy tracking tool is explained for the eddy core in Sect. 4.1 and the eddy size and shape in Sect. 4.3.

4 ~~Euler-Lagrangian~~ The Lagrangian descriptor M_V as eddy tracking tool

The mean oceanic flow is superimposed by many eddies of different sizes which emerge at some time instant, persist for some time interval and disappear. Consequently, an eddy tracking tool has to detect them at the instance of emergence, track them over their lifetime and detect their disappearance. To classify the different eddies some information about their size is needed too. This way one can finally obtain the time evolution of a size distribution function of eddies.

In this section we apply the ~~Euler-Lagrangian~~ modulus of vorticity based Lagrangian descriptor M_V to the ~~hydrodynamical~~ hydrodynamic model of a vortex street to test its performance as an eddy tracking tool. We use ~~its characteristics that it displays the centres of the eddies (elliptic fixed points) as local maxima and allows simultaneously the identification of invariant manifolds in~~ the ~~flow which in combination with the Lagrangian descriptor M will serve as estimators~~ local maxima of M_V for an automated search for eddy cores and in addition, the area enclosed by the singular lines of M_V associated with the manifolds of the DHTs as measure for the size of the eddies.

4.1 Eddy birth and lifetime

~~We ask~~ First we check how well M_V ~~predicts the lifetime~~ detects the birth of an eddy and ~~the time instant of the eddy birth~~ its lifetime and compare the results to the oceanographic eddy tracking tool box (ETTB) by Nencioli et al. (2010), as well as Eulerian quantities like the Okubo-Weiss parameter and the modulus of vorticity.~~As pointed out in the previous section the Lagrangian descriptor M cannot be used as an eddy tracking tool because it does not distinguish between elliptic and hyperbolic fixed points. However, it will be used to determine the size of the eddy, once it has been detected using the Euler-Lagrangian descriptor M_V.~~

The idea of the tracking inspired by Nencioli et al. (2010) is to search for local maxima (M_V and modulus of vorticity) or local minima (Okubo-Weiss, velocity based method by Nencioli et al. (2010)) surrounded by a region of gradient towards the maximum or minimum in a given search window~~that is shifted to the region of interest~~. The size of the search window determines which maximal eddy ~~sizes~~ size can be detected. The eddy is tracked from one time step to the ~~other~~ next by searching for an eddy core with the same direction of rotation within a given distance. The choice of this distance depends on the velocity field. It should be in the range of the maximal distance a particle could travel in the timespan of interest. The position of an eddy is logged in a track-list for each eddy at each time step. ~~To give a criterion when an eddy track is completed or to avoid false positive tracks or tracks of short living eddies one is not interested in, a threshold number of time steps should be defined.~~ A track-list ~~of an eddy that is not longer updated for this number of time steps is closed. A track-list that is shorter than the~~ that is shorter than a given threshold number of time steps is deleted to focus on eddies which exist longer than this minimum time interval. A detailed description of the ~~algorithm~~ algorithms can be found in the supplemental material to this article.

In order to check the accuracy of the eddy tracking algorithm, we use the dimensionless model of the vortex street presented in Sect. 3~~in a dimensionless parametrization~~, since the time instant of birth of the eddies and their lifetimes are given analytically. We ~~measured~~ measure both quantities for different dimensionless lifetimes T_c and dimensionless vortex strengths of 200, 100 and 50 for the eddy that arises at time $T_c/2$. The ~~rational~~ rationale behind varying the vortex strength is to estimate how weak an eddy could be to ~~have still a reliable detection by the method~~be still reliably detected by the methods. For M_V, τ was chosen as $0.15 \cdot T_c$. The results are presented in Figs. 4 and 5.

In all cases independent of the vortex strength, the results obtained with M_V are close to the analytical T_c (Fig. 4) or the analytical time instant of birth (Fig. 5). All other methods underestimate T_c and overestimate the time instant of birth. Especially in case of ~~the eddy tracking tool box (ETTB) by Nencioli et al. (2010)~~ ETTB the estimated times depend heavily on the vortex strength. ~~It~~ For that method it becomes more and more difficult to detect the eddy as ~~the~~ its rotation speed decreases. The reason for the good estimates provided by M_V ~~is that by construction M_V~~ lies in its construction which makes use of the history of the eddy (past and future). Hence it can detect eddies earlier than they arise by taking into account the future or detect them longer than they actually exist by looking into the past. M_V is not restricted to the information about the velocity field at one instant of time like the other methods. However, the performance of M_V depends on the chosen value of τ (Fig. 6). If τ gets too large in relation to T_c, the estimate of the lifetime deviates from the analytical one because the trajectories contain too much of the

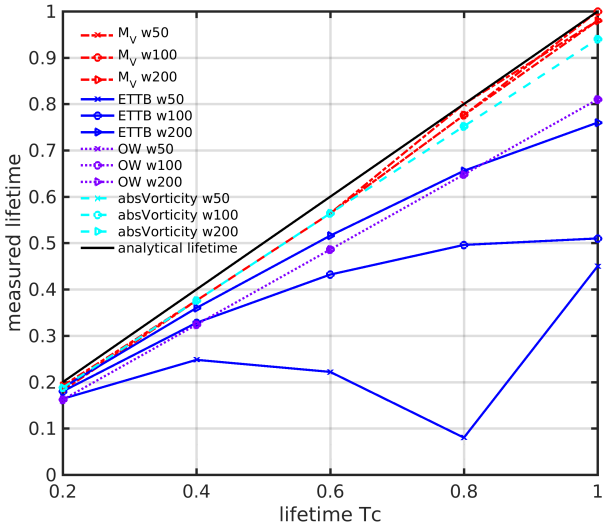

Figure 4. Eddy lifetime estimated with Okubo-Weiss (OW), modulus of vorticity (absVorticity), M_V and the eddy tracking tool box (ETTB) by Nencioli et al. (2010) for vortex strength w 50, 100 and 200. The black diagonal depicts the analytical lifetime.

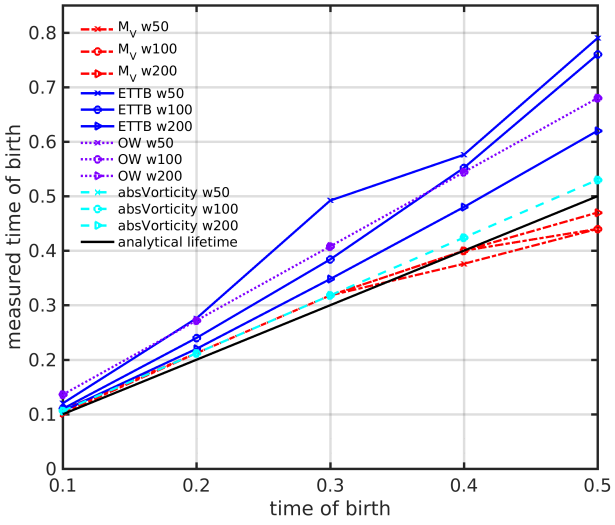

Figure 5. Time of birth of an eddy estimated with Okubo-Weiss (OW), modulus of vorticity (absVorticity), M_V and the eddy tracking tool box (ETTB) by Nencioli et al. (2010) for vortex strength w 50, 100 and 200. The black diagonal depicts the analytical time of birth of an eddy.

history of the eddy. There exists ~~an~~ a small range of optimal τ for a certain class of eddies. ~~A good choice in our case is~~ In our case the range is between about 15 % and 18 % of the eddy lifetime~~other application~~. We have chosen 15 % of the eddy

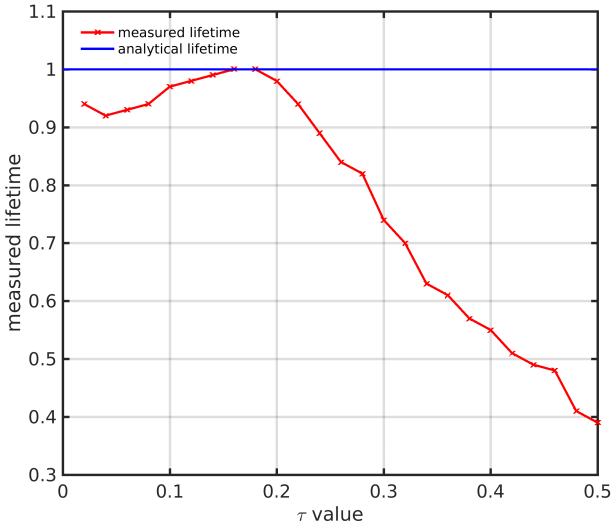

Figure 6. Measured lifetime of an eddy obtained by means of M_V versus the chosen τ (analytical lifetime $T_c = 1$ (blue line), vortex strength 200).

lifetime, because larger τ values increase the computational costs for M_V, too. The range of the optimal τ depends crucially on the application. Other applications might need a larger or smaller τ ~~.~~ or a τ that is a compromise between structures with very different lifetimes. It is also advisable to vary τ to detect different size and lifetime spectra of eddies.

4.2 Robustness of the lifetime detection with respect to noise

Velocity fields describing ocean flows have either a finite resolution when obtained by simulations or contain measurement noise when retrieved from observational data. For this reason, an eddy tracking method has to be robust with respect to fluctuations of the velocity field. ~~For this reason we will~~ Therefore, we explore how the detected eddy lifetime depends on noise ~~in~~ added to the velocity data.

~~We use three types of noise based on the different sources of noise~~ To test the influence of noise in a manageable test setup where we know all parameters like e.g. eddy lifetime (here $T_c = 1$) or vortex strength (here $w = 200$) we use the velocity components $u(x,y,t)$ and $v(x,y,t)$ of the vortex street mentioned in Sect. 3 and add three different types of noise to it mimicking measurement noise that can arise in observations~~or simulations~~. The result are noisy velocity components $u_N(x,y,t)$ and $v_N(x,y,t)$ for which we calculate Okubo-Weiss, modulus of vorticity and M_V and then apply the different eddy tracking methods. The noise is realised as white Gaussian noise in form of a matrix of normally distributed random numbers of the grid size for each time step multiplied by a factor that is referred to as noise level or noise strength. The noise level is given dimensionless, because the noise is applied to the dimensionless model of the vortex street presented in Sect. 3. The different noise types and their motivation are given in the following:

1. type 1: We add white Gaussian noise $\xi(x,y,t)$ of different noise strength σ between 0.05 and 0.95 to the velocity ~~field~~ components $u(x,y,t)$ and $v(x,y,t)$ of the vortex street~~with analytical eddy lifetime $T_c = 1$ and vortex strength $w = 200$~~. The noise is uncorrelated in space and time. The ~~velocity field~~ resulting velocity components $u_N(x,y,t) = u(x,y,t) + \sigma \cdot \xi_u(x,y,t)$ and $v_N(x,y,t) = v(x,y,t) + \sigma \cdot \xi_v(x,y,t)$ in this case ~~is~~ are still periodic but noisy. This type of noise mimics the effect of computing derivatives of observed velocity fields (e.g. by satellites or HF-radar).

2. type 2: We add ~~multiplicative~~ white Gaussian noise $\xi(x,y,t)$ of different noise strength σ between 0.05 and 0.95 to the velocity ~~field~~ components $u(x,y,t)$ and $v(x,y,t)$ of the vortex street but take into account that the actual noise depends on the velocity itself by taking the maximum of it over the whole spatial grid. The motivation is that the strength of noise depends on the ~~"~~"Signal to noise~~"~~" ratio. If we have a strong current, it is easy to detect this by a satellite, since the signal-strength is high. This is opposite for slow currents, where the noise level is much higher. Thus, we add white noise that is inversely proportional to the current speed~~in the sense of noise/(1+maximum of the current speed).~~. The noisy velocity components are given as $u_N(x,y,t) = u(x,y,t) + \sigma \cdot \xi_u(x,y,t)/(1 + \max_{x,y}(u(x,y,t)))$ and $v_N(x,y,t) = v(x,y,t) + \sigma \cdot \xi_v(x,y,t)/(1 + \max_{x,y}(v(x,y,t)))$.

3. type 3: We add white Gaussian noise $\xi(t)$ of different noise strength σ between 0.05 and 0.5 to the y-component of the eddy centres' movement. The equations of the unperturbed velocity field contains a part that describes the movement of the eddy centres (see supplemental material). The motion of the y-components of the eddy centres in the unperturbed velocity field (u, v) is given by $y_1(t) = y_0 = -y_2(t)$ where the index 1or 2 refers to the two eddies. The movement of the eddy centres in case of noise is given by $y_{1N}(t) = y_0 + \sigma \cdot \xi(t)$ and $y_{2N}(t) = -y_0 + \sigma \cdot \xi(t)$. This type of noise can be observed if the velocity fields have to rely on georeferencing. For instance, satellite generated velocity fields have to be mapped on a longitude/latitude grid, since the satellite is moving. During this postprocessing step a shift in the georeference is possible, leading to translational shifts and thus to type 3 noise. However, a high noise level of type 3 is not very likely. If one deals with typical geophysical applications, which have a grid resolution of the order 1 to 10 km, the georeferencing errors are mostly small compared to the grid cell size. ~~We have applied noise of type 1, 2 and~~ For this reason, the considered noise levels for type 3 ~~to the dimensionless model of the vortex street presented in Sect. 3. We have used~~ noise are smaller than for type 1 and 2.

To explore the impact of noise systematically, we have used different noise strengths. For each noise strength σ 1000 realizations of the white Gaussian noise ~~per noise strength and~~ were calculated. In the resulting velocity fields we estimated the lifetime of each eddy that undergoes a whole life-cycle within the ~~time of simulation~~ simulation time. The plotted eddy lifetimes obtained with all different tracking methods are medians of the distributions of the lifetimes for the 1000 realizations per noise strength (Fig. 7, 8, 9).

The three types of noise illustrate different advantages and disadvantages of M_V compared to the other methods. In case of type 1 noise, M_V gives the best estimate of the lifetime compared to ~~the~~ all other methods independent of the increasing noise level. The reason why the error of the estimate in case of M_V does not increase with increasing noise level is that M_V is a measure that is based on an integral. ~~It accumulates the~~ Integrating over accumulated uncorrelated noise along the trajectory

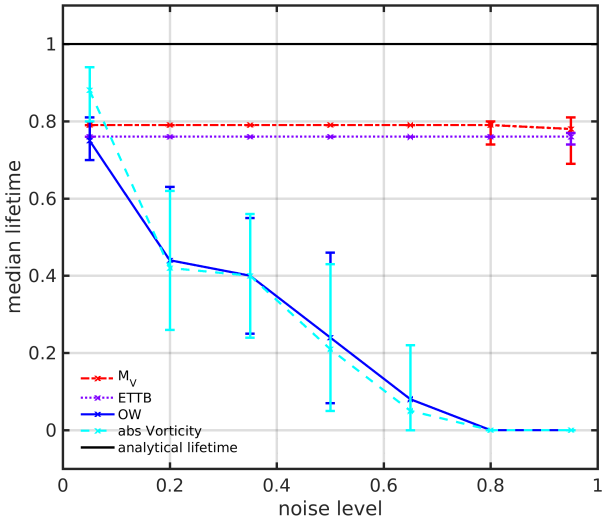

Figure 7. Measured median lifetime obtained by different methods (Okubo-Weiss (OW), modulus of vorticity (absVorticity), M_V and the eddy tracking tool box (ETTB) by Nencioli et al. (2010)) depending on the noise level. The computations have been performed in a velocity field mimicking a vortex street with added white Gaussian noise (type 1 noise with 1000 noise realizations). The errorbars indicate the whiskers of the distribution in the boxplot (not shown here) corresponding to approximately $\pm 2.7\sigma$.

from past to future ~~. Integrating over this accumulated noise~~ can be considered as a smoothing process. Also the ~~method~~ ETTB by Nencioli et al. (2010) gives a good result independent of the increasing noise level, because the signal to noise ratio is small. The minimum of the velocity that is the key-signal for determining the eddy core in their method ~~is still~~ remains a local minimum in the contour plot of the velocity. However, with increasing noise level we ~~see~~ find an increase of outliers for the ~~method~~ ETTB by Nencioli et al. (2010) and M_V (boxplot not shown here)~~of the data of the method~~ . The performance of modulus of vorticity and the Okubo-Weiss parameter decreases as expected with increasing noise level while the distribution increases in width (Fig. 7). The reason is that the noise gets so large that it increasingly disturbs the key-signal for an eddy core until no distinct eddy core can be identified anymore.

In case of type 2 noise, M_V and ~~the method by Nencioli et al. (2010)~~ ETTB show a similar behaviour as in case of type 1 noise. Both yield good results independent of the noise level. This is again due to the smoothing process in case of M_V. The modulus of vorticity ~~gives results that are~~ performs even better than M_V in case of small noise levels, but its performance drops below the results of M_V with increasing noise level (Fig. 8). The reason is that the key-signal for determining an eddy core using the modulus vorticity is stronger in case of small noise levels and gets disturbed by the noise with increasing noise level. ~~By contrast, the smoothing process in M_V is the same independent of the noise level. As expected~~As expected, the performance of Okubo-Weiss decreases with increasing noise level. In contrast to type 1 noise, Okubo-Weiss can identify eddy cores even in case of strong noise~~eddy cores can be identified~~ , because the key-signal for an eddy core is less disturbed.

In case of type 3 noise, M_V yields an estimate of the lifetime with the largest error (Fig. 9). ~~The reason is that in~~ In this case

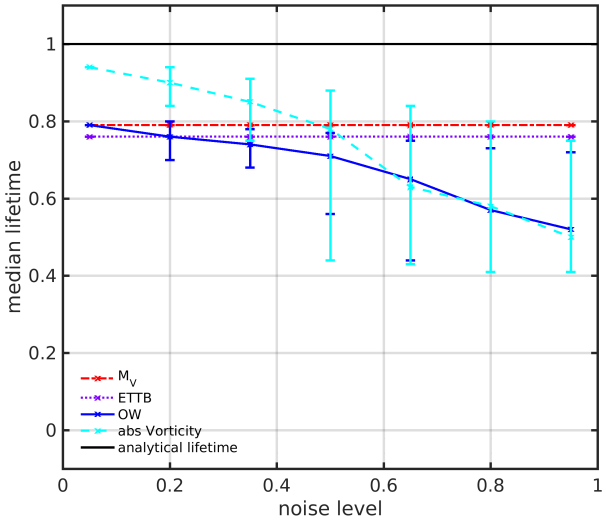

Figure 8. Measured median lifetime obtained by different methods (Okubo-Weiss (OW), modulus of vorticity (absVorticity), M_V and the eddy tracking tool box (ETTB) by Nencioli et al. (2010)) depending on the noise level. The computations have been performed in a velocity field mimicking a vortex street with type 2 noise (1000 noise realizations). The errorbars indicate the whiskers of the distribution in the boxplot (not shown here) corresponding to approximately $\pm 2.7\sigma$.

noisy trajectories that start close to each other diverge fast, while the ones with no noise have a similar dynamical evolution. This divergence due to noise leads to a loss of structure in space ~~which~~ that can be interpreted as a weakening of the correlation between neighbouring trajectories. This effect is strongest in case of M_V because it integrates over time and so neighbouring trajectories that have similar values of M_V in case of no noise yield very different values of M_V due to the divergence of the trajectories. As a consequence no clear structure in M_V can be identified. This effect increases with the noise level.

Also for the other methods noise of type 3 affects strongly the identification of the eddy core because the weakening of the correlation between neighbouring points disturbs the key-signal of an eddy core (a local minimum or maximum in a certain domain). The error in estimating the lifetime increases with increasing noise level. In all cases the number of outliers in the boxplot (not shown here) increases with the noise level.

As a ~~result, non~~ consequence, none of the methods performs in an optimal way when the noise ~~affects the movement of the eddy cores~~ displaces the eddy cores during their motion. This disadvantage will lead to deviations in the lifetime statistics for eddy tracking based on observational data. However~~nowadays~~, the error in georeferencing of satellite images (which is mimicked by type 3 noise) is mostly small. For special applications, a georeferencing error of smaller than 1/50 pixel is achievable (Leprince et al. (2007)). Eugenio and Marqués (2003) show that with reasonable effort a mapping error smaller than 0.5 pixel is possible, if fixed landmarks (coastlines, islands) are on the images. With the increase in earth orbiting satellites and thus the increase in available images, it can be assumed that this error will drop even more (Morrow and Le Traon (2012)). ~~Anyhow~~If numerically generated velocity fields are used, noise of type 3 is completely absent~~, if numerically generated velocity fields are~~

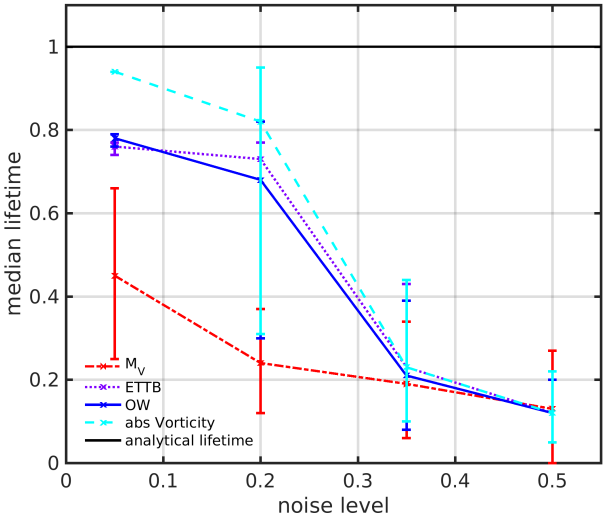

Figure 9. Measured median lifetime obtained by different methods (Okubo-Weiss (OW), modulus of vorticity (absVorticity), M_V and the eddy tracking tool box (ETTB) by Nencioli et al. (2010)) depending on the noise level. The computations have been performed in a velocity field mimicking a vortex street with type 3 noise (1000 noise realizations). The errorbars indicate the whiskers of the distribution in the boxplot (not shown here) corresponding to approximately $\pm 2.7\sigma$.

~~used~~. Here the evolution of neighbouring trajectories ~~are~~ is smooth and correlated.

In summary, M_V can be used for the detection of eddies and the estimate of eddy lifetimes for velocity fields with and without noise and yields good results independent of the noise level in case of type 1 and 2 noise. However, one has to take into account that the velocity field should not be too noisy and that one has to chose a τ that fits the problem. The ~~Euler-Lagrangian~~ Lagrangian descriptor M_V has an additional advantage in detecting arising eddies earlier than other methods due to collecting information along the trajectory from past to future. This can be useful in the identification of regions that will be eddy dominated in the further evolution of the flow.

4.3 Detecting eddy sizes and shapes

Beside its lifetime an eddy is characterized by its ~~shape~~size. In the following we will estimate the eddy ~~shape using a combination of the vorticity-based Euler-Lagrangian~~ size and shape using the the Lagrangian descriptor M_V ~~and the arc-length based Lagrangian approach M. We~~ based on the modulus of vorticity and compare the results to the ~~shapes~~ size detected by the ~~eddy tracking tool~~ ETTB by Nencioli et al. (2010). In this way, we demonstrate the differences between the Eulerian and ~~Euler-Lagrangian~~ Lagrangian point of view on the eddy size and shape.

~~From the Euler-Lagrangian point of view the~~ As mentioned in Sect. 2 the estimation of the eddy shape and size from the Lagrangian point of view is based on the idea that the boundaries of the eddy are linked to manifolds of DHTs that surround the eddy ~~. This idea has been formulated by Bettencourt et al. (2012), who point out, that eddies are bounded by invariant~~

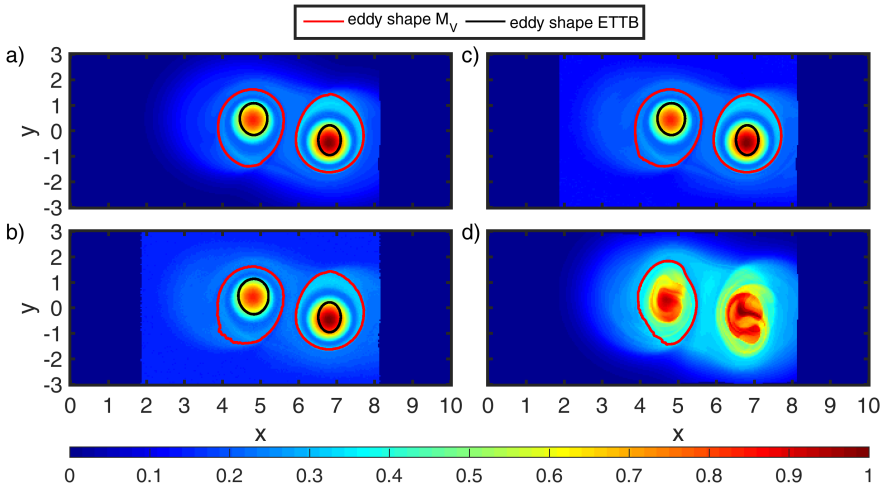

Figure 10. Eddy ~~shape~~ boundaries detected with the method based on ~~M and~~ M_V (red line) and with the eddy tracking tool by Nencioli et al. (2010) (black line) at ~~$t = 0.151$~~$t = 0.201$. ~~The color code indicates:~~ (a) ~~M~~ M_V without noise, (b) ~~M~~ M_V with type 1 noise of noise level 0.95, (c) ~~M~~ M_V with type 2 noise of noise level 0.95, (d) ~~M~~ M_V with type 3 noise of noise level 0.5. The τ value is chosen as 0.15 T_c with $T_c = 1$. The dark blue regions are regions where the trajectories have left the region of interest. All plots are normalized to the maximum value.

~~manifolds surrounding the eddy and acting as transport barriers.~~ (Branicki et al. (2011); Bettencourt et al. (2012)). These manifolds cannot be crossed by any trajectories and, therefore, trajectories starting inside the manifolds are trapped in the eddy. Defining the boundaries in this way one can estimate the trapping region or volume that is transported by an eddy.

The ~~shape detection algorithm combines the Lagrangian descriptor M and the Euler-Lagrangian~~ Lagrangian descriptor M_V ~~and searches for~~ displays singular lines that correspond to manifolds. Therefore, the shape detection algorithm searches for the largest closed contour ~~lines with the local lowest level of M which surrounds the elliptic fixed point~~ line of M_V for which M_V is an extremum and which surrounds an eddy core found with M_V. This ~~line is~~ contour line, extracted from M_V with the MATLAB function contourc and along which the gradient of M_V is large, should be a line on or ~~close to the manifold displayed by M or~~ very close to a singular line displayed by M_V ~~. By contrast, the eddy tracking tool~~ corresponding to a manifold and will give an estimate of the eddy boundary.

The ETTB by Nencioli et al. (2010) gives an Eulerian view on the eddy shape by defining the eddy boundaries as the largest closed streamline of the streamfunction around the eddy centre where the velocity still increases radially from the centre. The contour lines as well as the streamlines are extracted in a given search window which is centred on the eddy core.

The comparison of the different views on the eddy size and shape is presented in Fig. 10 for the vortex street without (a) and with noise of type 1, 2 and 3 (b-d). ~~As expected the shape~~ The size detected with the ~~eddy tracking tool~~ ETTB by Nencioli et al. (2010) is much smaller than the ~~shape~~ size based on the ~~Euler-Lagrangian~~ Lagrangian view (Fig. 10 a-c). Additionally, the evolution of the eddy is captured by both methods even in case of strong type 1 and 2 noise (Fig. 10 b and c). ~~The shape~~

computed by the combination of M and Here, the eddy boundaries in case of noise show small irregularities due to the noise. In general, the eddy boundary computed based on M_V is detected earlier and shows more growing and shrinking during the evolution of the eddy than the eddy boundary extracted by the ETTB. This is due to the conceptual idea of the measure M_V that contains the history of the trajectories. As shown in Sect. 4.2 this concept of M and M_V leads to problems in case of a velocity field with type 3 noise (although significant type 3 noise levels are very unlikely). If the noise level is too largeno structure , no structure neither a clear eddy core nor a clear eddy boundary can be detected (Fig. 10 d) with M and within M_V. But if an eddy core can be detected as in case of the left eddy in Fig. 10 (d) the eddy shape detection based on M_V gives an idea of the size and the noisy eddy boundary.

In a real oceanic flow eddies of different lifetime, size and shape will occur simultaneously. To illustrate As an outlook, how different eddy shapes and sizes can be detected in real oceanic flow fields, we apply our approach to a seeded eddy model that mimics such an oceanic eddy field . The model is inspired by velocity field of the western Baltic Sea for May 2009. The Baltic Sea is a good testbed, since the tides there are negligible and the entire eddy dynamics is driven by baroclinic instabilities, frontal dynamics and the interaction with topography. An extended eddy statistics in the central Baltic Sea based on M_V will be the content of further research.

A triple-nested circulation model was used to simulate the flow fields in the seeded eddy model of a turbulent flow described in Abraham (1998) and the model of Jung et al. (1993) to elucidate the role of eddies in the formation of plankton patchiness. The model consist of a background flow of $0.18\ \mathrm{ms}^{-1}$ and ten mesoscale eddies of different sizes. Their radii r are drawn from a distribution possessing a power law $1/r^3$ where the minimal radius is 10 km and the maximal radius is western Baltic Sea. The innermost model domain was discretised in the horizontal with a spatial resolution of 1/3 nautical mile (approx. 600 m). The model domain covers the Danish Straits and the western Baltic. The open boundaries are located in the Kattegat and at the eastern rim of the Bornholm Basin. In the vertical 50 km. Because we are interested in mesoscale eddies, the drawn radii are between 15 km and 25 km. One half of the eddies rotates clockwise and the other half counter-clockwise. Their position in space is drawn from an uniform distribution. To generate a dimensionless model, lengths are measured in units of the maximal eddy radius of the mesoscale eddies and timein units of the lifetime of an eddy which is chosen equally for all eddies ($T_c = 1$). τ is chosen as 0.15. A detailed description can be found in the supplemental material to this article.terrain-following adaptive layers, with a zooming toward stratification were used. The setup is identical to the one used by Klingbeil et al. (2014) or Gräwe et al. (2015b). There, a detailed description and validation of the present setup can be found. At the open boundaries of the model domain, the water elevations, depth averaged currents, as well as salinity and temperature profiles are prescribed. This external forcing was taken from a model of the North Sea-Baltic Sea with a horizontal resolution of 1 nautical mile and 50 vertical layers. To account for large scale variations and remotely generated storm surges, the North Sea-Baltic Sea model was nested into a depth-averaged storm surge model of the North Atlantic with a resolution of 5 nautical miles. The atmospheric forcing was derived from the operational model of the German Weather Service with a spatial resolution of 7 km and temporal resolution of 3 hours. A more detailed description of the model system is given by Gräwe et al. (2015a). The flow fields for May 2009 were taken out of a running simulation covering the period 1948-2015. The velocity field was interpolated to an

~~M normalized to the maximum value with the eddy shapes of the seeded eddy model detected with the method based on M and M_V (red lines) and with the eddy tracking tool by Nencioli et al. (2010) (black line). τ is chosen as 0.15 T_c with $T_c = 1$. The dark blue regions are regions where the trajectories have left the region of interest.~~

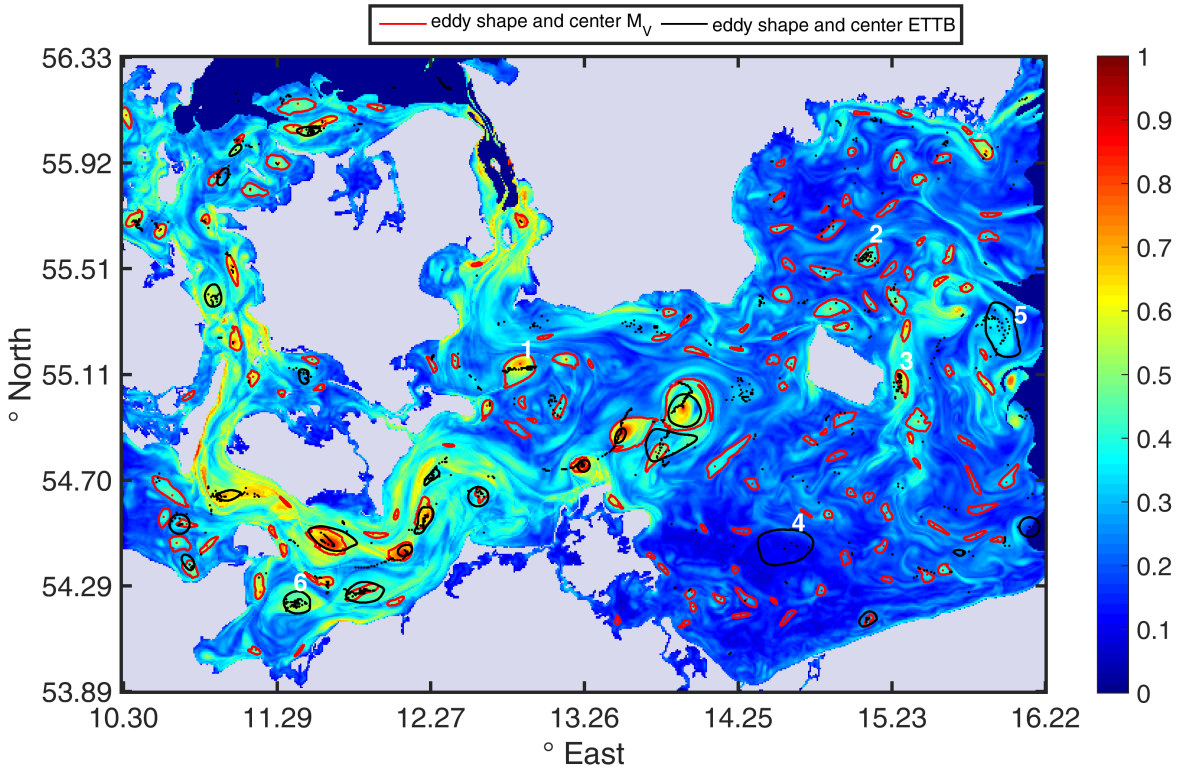

Figure 11. M_V for the western Baltic Sea for 11 May 2009 1:00 am with $\tau = 36$ h normalized to the maximum value of M_V. The red lines are the eddy boundaries and red dots the eddy cores detected with the method based on M_V respectively. The black lines are the eddy boundaries detected with the ETTB by Nencioli et al. (2010) at 11 May 2009 1:00 am. The black dots are the eddy cores detected with the ETTB by Nencioli et al. (2010) within the time interval 11 May 2009 1:00 am $\pm$36 h. The dark blue regions are areas where the trajectories have left the domain of interest, light grey regions indicate land.

equidistant spacing of 1 m and finally averaged over the upper 10 m to produce a "quasi" two-dimensional field. The temporal resolution was set to one hour to resolve for instance inertial oscillations. ~~The result is presented~~

We have calculated M_V for 11 May 2009 1:00 am with $\tau = 36$ h and applied the eddy tracking based on M_V. A τ value of 36 h corresponds to 15 % of an eddy lifetime of approx. 10-12 days, which was reported previously by Fennel (2001). In contrast to the test case of the vortex street, we do not expect that the eddies are perfectly circular. To account for deformed and distorted eddies, we had to introduce a threshold for the convexity deficiency to eliminate contours that are only made out of filaments and are no eddy in the sense of oceanography. We set the threshold to 11% difference between the area of the convex hull of the points that form the boundary and the area enclosed by the boundary itself normalised to the area enclosed of the

boundary. This definition of convexity deficiency is according to Haller et al. (2016). Please note, that we still allow to detect contours that cover eddy merging and decay processes, which are characterized by filaments.

Fig. 11 shows the eddy boundaries detected with the method based on M_V (red) and the ETTB by Nencioli et al. (2010) (black) at 11 May 2009 1:00 am for the same search window size. There are several differences between the number and shapes of eddies which has to be explained. 150 eddies can be detected with the method based on M_V, whereas the ETTB detects only 24 eddies at the same instant of time. One reason for the differences is that M_V contains the information of the velocity field of a time interval, namely 11 May 2009 1:00 am $\pm$36 h. Each eddy that exists, starts to arise, merges with another eddy or dies within this time interval leaves a footprint in M_V like the many of small eddies visible in M_V. How strong this footprint is visible in M_V depends on the choice of τ. Therefore, the number of eddies detected with the method based on M_V has to be compared with the number of eddies detected with the ETTB by Nencioli et al. (2010) in the whole time interval that is covered by M_V.

The black dots in Fig. 11 ~~. As expected the eddy shapes are larger in case of M and M_V than in case of the eddy tracking tool by Nencioli et al. (2010) since both approaches use different definitions of the eddy shape.A problem arises in case of M and~~ are the eddy cores detected with the ETTB by Nencioli et al. (2010) within the time interval 11 May 2009 1:00 am $\pm$36 h. In total, 339 eddies are detected which exist between less than one hour and 72 hours. For some eddies we will discuss exemplarily why they are detected by one of the methods and not by the other to illustrate which different problems have to be taken into account if one interprets the results of the different methods.

Close to or within the eddy 1, 2 and 3 detected by the tracking based on M_V ~~if the eddy boundaries are too close to each other (Fig. 11 upper right eddies). The eddy tracking~~ are several eddy cores detected by the ETTB by Nencioli et al. (2010) if one takes into account the whole time interval. At 11 May 2009 1:00 am the ETTB does not detect eddy 1, 2 and 3 because they are to weak or do not exist yet. By contrast, the eddy detection method based on M_V detects ~~the~~ them due to the construction of M_V as an integral over time. For eddy 4 only a few eddy cores are detected by the ETTB by Nencioli et al. (2010) for the whole time interval, probably the eddy is to weak and lives to short to be seen as a structure in M_V. In case of eddy ~~cores and identifies the eddies as separated. However the filaments of the~~ 5 the method based on M_V does not detect an eddy although the ETTB by Nencioli et al. (2010) detects several eddy cores in the region. One reason could be that the eddy arises, moves a lot and dies within the time interval such that M_V only captures a blurred structure of the eddy ~~boundary of one eddy are close to the boundary of the other eddy . The criterionto identify an~~ that does not fulfil the convexity criterion. Eddy 6 is not detected by the method based on M_V, although the eddy boundary is ~~to detect the largest closed contour line with the local lowest level of M within a search window . If the boundaries are close to each other any lowest local level of M within~~ obvious in the structure of M_V. The reason is that the choice of the search window size for the eddy core detection determines if an eddy core is detected or not. An enlarged search window could solve this problem for eddy 6, but a larger search window influences the number of detected eddies. A solution could be an eddy core search independent of the search window ~~can be clearly identified.~~size.

A general problem, which arises when using surface velocity fields, is that this velocity field is not divergence free. Although, we have checked that the vertical velocity is small compared to the horizontal ones, there is still a finite residual left. However,

~~note that this test case is rather artificial. Eddies are placed randomly in the ocean and eddy-eddy interaction is not taken into account. In realistic applications, if eddies are too close to each other, they certainly will interact, merge, or repel each other. Hence, the eddy tracking algorithm might still give reliable results~~we still assume that the velocities are two dimensional. Applying the ETTB by Nencioli et al. (2010) to these "quasi" 2d fields does not cause difficulties, since the algorithm works on an instantaneous snapshot - a frozen velocity field. Thus, the error made by the 2d assumption is small. The situation changes when employing a Lagrangian descriptor. During the integration interval $[t^* - \tau\, t^* + \tau]$, M_V accumulates these residuals. Therefore, M_V can show structures that seems to be eddies but are regions of a stronger vertical velocity or Lagrangian divergence (Jacobs et al. (2016)). Therefore, the number of eddies of both methods will include false positives.

In summary, the method based on the ~~combination of the Lagrangian descriptor M and the Euler-Lagrangian~~ Lagrangian descriptor M_V can be used for the detection of eddy boundaries that are acting as boundaries of a trapping region. Comparing the latter to boundaries detected with the ~~method~~ ETTB by Nencioli et al. (2010) leads to large differences in the shape ~~computed by both methods. Those differences~~ and in the size. Those deviations are due to the difference in the definition of the boundary and yields in case of the vortex street much smaller sizes of the eddies in case of the ~~eddy tracking tool~~ ETTB by Nencioli et al. (2010). Another advantage of the method based on the ~~combination of the Lagrangian descriptor M and the Euler-Lagrangian~~ Lagrangian descriptor M_V is that it even shows filament structures of the eddy boundary in contrast to the ~~method by Nencioli et al. (2010)~~ ETTB by Nencioli et al. (2010) visible in the example of the western Baltic Sea. These filaments can be linked to the dynamics of the eddy, e.g. as it starts interacting, merging, or repelling with other eddies or fading out. ~~Nevertheless~~ Though these filamental shapes of eddies might not be eddies according to a more strict mathematical definition of an eddy boundary as in Branicki et al. (2011); Haller et al. (2016), but they are still important structures in the flow from an oceanographic point of view and should be considered in a census of eddies.

Nevertheless, one has to take into account that the detection of eddy shapes by the method based on the ~~combination of the Lagrangian descriptor M and the Euler-Lagrangian~~ Lagrangian descriptor M_V is restricted by the ~~unlikely case of type 3 noise in velocity fields .~~

choice of τ. In highly dynamical velocity fields like the example of the Baltic Sea not all structures can be resolved by the same τ which leads to a compromise for τ. This choice of τ influences if an eddy can be detected by the method based on M_V and not by the ETTB by Nencioli et al. (2010) or the other way round.

The method to detect shapes should be chosen based on the question which type of shapes one is interested in and the results of the method should be handled with care.

5 Discussion and conclusion

We have shown, that the ~~introduced heuristic Euler-Lagrangian~~ Lagrangian descriptor M_V ~~provides a good insight in the flow~~ based on the modulus of vorticity provides good insights into the structure of a hydrodynamic ~~system. It identifies elliptic fixed points that can be linked to eddy cores and, in contrast to Eulerian measures,~~ flow. It can be used to identify eddy cores as well as distinguished hyperbolic trajectories. Eddy cores can be found as local maxima of M_V ~~even identifies hyperbolic fixed points.~~

Moreover it can distinguish between elliptic and hyperbolic fixed points - a property which cannot be achieved by , while DHTs correspond to minima of M_V. Hence, compared to the Lagrangian descriptor M . Therefore, the Euler-Lagrangian descriptor M_V is a suitable tool for tracking eddies and subsequently estimating their lifetimes. Like the Lagrangian descriptor M, M_V displays based on the arc length, it does not need an additional criterion to distinguish between eddy cores and DHTs. As any other Lagrangian descriptor it displays singular lines that can be linked to the stable and unstable manifolds and provides as an add-on estimates of the eddy boundaries. This fact linked to the idea that manifolds cannot be crossed by trajectories yields a different approach to the tracking of eddy shapes compared to an Eulerian method. Eulerian methods like the one of Nencioli et al. (2010) define the eddy boundary as a line with special properties of the velocity which cannot be linked to of the idea of trapping of fluid parcels inside the eddy DHTs which allows for a simultaneous estimate of the boundaries of the eddies to get an assessment of their size and shape. These features make the quantity M_V suitable for designing an eddy tracking tool, which should be able to detect eddy cores, to track them over time, and additionally to provide information about the eddies' lifetime, size and shape. Moreover, the eddy tracking should be robust with respect to velocity fields corroborated with errors in case the velocity field is extracted from observations.

We have demonstrated using some paradigmatic velocity fieldsthat the proposed Euler-Lagrangian descriptor M_V yields good results in estimating the To test all those properties in practice we have first used some velocity fields, which are constructed in such a way that the lifetimes of eddies and in combination with are given analytically. It turns out, that the Lagrangian descriptor M eddy shapes. Therefore, it is a suitable tool for eddy tracking in oceanic velocity fields. The Euler-Lagrangian descriptor M_V gives an estimate of the lifetime that is closest to the analytical lifetime (in the case of the vortex street), therefore it performs much better than any of the other methods in the comparison. It finds eddies earlier than the other methods because is superior in estimating lifetimes compared to the other considered methods. This is due to its definition as an integral which takes the history into account. Eulerian methods like Okubo-Weiss or the ETTB by Nencioli et al. (2010) detect eddies too late and underestimate their lifetime. The formulation of M_V contains information of the future and the past of the velocity field. This property can be useful if one is interested in the process of the eddy birth and its early evolutionas an integral is also beneficial in case of different types of noise. However, there are some disadvantages of this method which need to be addressed.none of the tested methods can deal in a convincing way with type 3 noise which mimics errors to shifts in georeferencing.

First of all, it is a heuristic method, that lacks objectivity. This can be problematic since it might lead to failures in the detection of some eddies. But it is easy to implement and fast, so that it compensates for this problem, when this measure is used for computing census and size distributions of eddies in oceanic flows over a long period of time.A general problem of the Lagrangian and the Euler-Lagrangian descriptors any Lagrangian descriptor including M and M_V is that the resolution of the structures to be detected depends on the chosen time τ. Structures that live too short in relation to the chosen τ cannot be resolved and will be missed. Hence the choice of τ contains a decision which time scale and subsequently which eddy lifetime will be resolved.We have shown that the Euler-Lagrangian descriptor

The example of the velocity field of the western Baltic Sea shows that eddy tracking based on M_V provides still good results if the velocity field is corroborated with noise of type 1 and 2. This is due to the smoothing effect inherent in the definition of M_V as an integral along the trajectory. The estimates of the eddy lifetime by M_V is in almost all cases better than the estimate of the

~~other methods. In case of velocity fields with strong type 3 noise collecting the history of the velocity field can be a drawback. As discussed in Sect. 4.2 type 3 noise leads to a divergence of neighbouring trajectories, which disturbs the structure of~~ able to detect the essential eddies that are visible in the velocity field and also detected by the ETTB by Nencioli et al. (2010). Furthermore, it detects eddies that cannot be detected by the ETTB at this instant of time t^*, but was or will be detected by the ETTB at a earlier or later instant of time within the time interval $[t^* - \tau\, t^* + \tau]$. Nevertheless, one has to be aware that both ETTB and the eddy tracking based on M_V ~~and in this way the detection of the eddy core or shape. A solution for this problem is the choice of a smaller time~~ give false positives. The reason could be that structures of strong vertical velocity are identified as eddies. On the other hand false negatives can arise if (i) the eddies are too weak or (ii) the chosen τ ~~to reduce the time span where the trajectories can diverge from each other. However, as discussed in Sect. 4.2 type 3 noise is very unlikely and completely absent, if numerical generated velocity fields are used~~value is too large or too small or (iii) the search window is too large or too small.

In general, the choice of the detection method depends on the questions asked. If one is only interested in tracking eddy cores Eulerian methods are a good choice. ~~Lagrangian and especially the Euler-Lagrangian method~~ By contrast, Lagrangian methods gives a more detailed view on the dynamics ~~. Besides, they~~ and provide a more physical estimate of the eddy size. Especially this feature, which describes the fluid volume trapped in an eddy promises to be more useful for applications that consider the growth of plankton populations in oceanic flows. For the latter it has been shown that eddies can act as incubators for plankton blooms due to the confinement of plankton inside the eddy (Oschlies and Garçon (1999); Martin (2003); Sandulescu et al. (2007)).

Author contributions. Rahel Vortmeyer-Kley developed the idea of the eddy tracking tool based on the Lagrangian descriptor M_V and implemented it. Ulf Gräwe supervised the oceanic questions of this work and provided the velocity field for the western Baltic Sea. The overall supervision was done by Ulrike Feudel. All authors contributed in preparing this manuscript.

Acknowledgements. Rahel Vortmeyer-Kley would like to thank the Studienstiftung des Deutschen Volkes for a doctoral fellowship. The financing of further developments of the Leibniz Institute of Baltic Sea Research monitoring program and adaptations of numerical models (STB-MODAT) by the federal state government of Mecklenburg-Vorpommern is greatly acknowledged by Ulf Gräwe.

The authors would like to thank Jan Freund, ~~Wenbo Tang and~~ Ana Mancho, Matthias Schröder, Wenbo Tang, Tamás Tél and Alfred Ziegler for stimulating discussions.

References

Abraham, E. R.: The generation of plankton patchiness by turbulent stirring, Nature, 391, 577–580, 1998.

Artale, V., Boffetta, G., Celani, M., Cencini, M., and Vulpiani, A.: Dispersion of passive tracers in closed basins: Beyond the diffusion coeffcient, Phys Fluids, 9, 3162–3171, 1997.

Bastine, D. and Feudel, U.: Inhomogeneous dominance patterns of competing phytoplankton groups in the wake of an island, Nonlinear Proc Geoph, 17, 715–731, 2010.

Bettencourt, J. H., López, C., and Hernández-García, E.: Oceanic three-dimensional Lagrangian coherent structures: A study of a mesoscale eddy in the Benguela upwelling region, Ocean Model, 51, 73–83, 2012.

Boffetta, G.and Lacorata, G., Redaelli, G., and Vulpiani, A.: Detecting barriers to transport: a review of different techniques, Physica D, 159, 58–70, 2001.

Bracco, A., Provenzale, A., and Scheuring, I.: Mesoscale vortices and the paradox of the plankton, P Roy Soc Lond B Bio, 267, 1795–1800, 2000.

Branicki, M. and Wiggins, S.: Finite-time Lagrangian transport analysis: stable and unstable manifolds of hyperbolic trajectories and finite-time Lyapunov exponents, Nonlinear Proc Geoph, 17, 1–36, 2010.

Branicki, M., Mancho, A., and Wiggins, S.: A Lagrangian description of transport associated with a front-eddy interaction: Application to data from the North-Western Mediterranean Sea, Physica D, 240, 282–304, 2011.

Chaigneau, A., Gizolme, A., and Grados, C.: Mesoscale eddies off Peru in altimeter records: Identification algorithms and eddy spatio-temporal patterns, Prog Oceanogr, 79, 106–119, 2008.

Chelton, D. B., Schlax, M. G., and Samelson, R. M.: Global observations of nonlinear mesoscale eddies, Prog Oceanogr, 91, 167–216, 2011.

de la Cámara, A., Mancho, A. M., Ide, K., Serrano, E., and Mechoso, C. R.: Routes of Transport across the Antarctic Polar Vortex in the Southern Spring, J Atmos Sci, 69, 741–752, 2012.

Dong, C., Idica, E. Y., and McWilliams, J. C.: Circulation and multiple-scale variability in the Southern California Bight, Prog Oceanogr, 82, 168–190, 2009.

Dong, C., Lin, X., Liu, Y., Nencioli, F., Chao, Y., Guan, Y., Chen, D., Dickey, T., and McWilliams, J. C.: Three-dimensional oceanic eddy analysis in the Southern California Bight from a numerical product, J Geophys Res, 117, C00H14, 2012.

Dong, C., McWilliams, J. C., Liu, Y., and Chen, D.: Global heat and salt transports by eddy movement, Nature Communications, 5, 1–6, 2014.

Donlon, C. J., Martin, M., Stark, J., Roberts-Jones, J., Fiedler, E., and Wimmer, W.: The Operational Sea Surface Temperature and Sea Ice Analysis (OSTIA) system, Remote Sensing of Environment, 116, 140–158, 2012.

Douglass, E. M. and Richman, J. G.: Analysis of ageostrophy in strong surface eddies in the Atlantic Ocean, J Geophys Res: Oceans, 120, 1490–1507, 2015.

d'Ovidio, F., Fernández, V., Hernández-García, E., and López, C.: Mixing structures in the Mediterranean Sea from Finite-Size Lyapunov Exponents, Geophys Res Lett, 31, L17 203, 2004.

Eugenio, F. and Marqués, F.: Automatic Satellite Image Georeferencing Using a Contour-Matching Approach, IEEE T Geosci Remote, 41, 2869–2880, 2003.

Fennel, K.: The generation of phytoplankton patchiness by mesoscale current patterns, Ocean Dynam, 52, 58–70, 2001.

Fernandes, M. A., Nascimento, S., and Boutov, D.: Automatic identification of oceanic eddies in infrared satellite images, Comput Geosci, 37, 1783–1792, 2011.

Froyland, G. and Padberg, K.: Almost-invariant sets and invariant manifolds - Connecting probabilistic and geometric descriptions of coherent structures in flows, Physica D, 238, 1507–1523, 2009.

Froyland, G., Horenkamp, C., Rossi, V., Santitissadeekorn, N., and Guptac, A. S.: Three-dimensional characterization and tracking of an Agulhas Ring, Ocean Model, 52, 69–75, 2012.

García-Garrido, V., Mancho, A. M., Wiggins, S., and Mendoza, C.: A dynamical systems approach to the surface search for debris associated with the disappearance of flight MH370, Nonlinear Proc Geoph, 22, 701–712, 2015.

Gawlik, E. S., Marsden, J. E., Du Toit, P. C., and Campagnola, S.: Lagrangian coherent structures in the planar elliptic restricted three-body problem, Celest Mech Dyn Astr, 103, 227–249, 2009.

Gräwe, U., Holtermann, P., Klingbeil, K., and Burchard, H.: Advantages of vertically adaptive coordinates in numerical models of stratified shelf seas, Ocean Model, 92, 56–68, 2015a.

Gräwe, U., Naumann, M., Mohrholz, V., and Burchard, H.: Anatomizing one of the largest saltwater inflows into the Baltic Sea in December 2014, J Geophys Res-Oceans, 120, 7676–7697, 2015b.

Haller, G.: Distinguished material surfaces and coherent structures in three-dimensional fluid flows, Physica D, 149, 248–277, 2001.

Haller, G.: Lagrangian Coherent Structures, Annu Rev Fluid Mech, 47, 137–162, 2015.

Haller, G. and Beron-Vera, F.: Coherent Lagrangian vortices: the black holes of turbulence, J Fluid Mech, 731, R4, 2013.

Haller, G. and Yuan, G.: Lagrangian coherent structures and mixing in two-dimensional turbulence, Physica D, 147, 352–370, 2000.

Haller, G., Hadjighasem, A., Farazmand, M., and Huhn, F.: Defining coherent vortices objectively from the vorticity, J Fluid Mech, 795, 136–173, 2016.

Hernández-Carrasco, I., Rossi, V., Hernández-García, E., Garçon, V., and López, C.: The reduction of plankton biomass induced by mesoscale stirring: A modeling study in the Benguela upwelling, Deep-Sea Res Pt I, 83, 65–80, 2014.

Huhn, F., Kameke, A., Pérez-Muñuzuri, V., Olascoaga, M., and Beron-Vera, F.: The impact of advective transport by the South Indian Ocean Countercurrent on the Madagaskar plankton bloom, Geophys Res Lett, 39, 2012.

Ide, K., Small, D., and Wiggins, S.: Distinguished hyperbolic trajectories in time-dependent fluid flows: analytical and computational approach for velocity fields defined as data sets, Nonlinear Proc Geoph, 9, 237–263, 2002.

Isern-Fontanet, J., García-Ladona, E., and Font, J.: Vortices of the Mediterranean Sea: An Altimetric Perspective, J Phys Oceanogr, 36, 87–103, 2006.

Jacobs, G. A., Huntley, H. S., Kirwan, A., Lipphardt, B. L., Campbell, T., Smith, T., Edwards, K., and Bartels, B.: Ocean processes underlying surface clustering, J Geophys Res-Oceans, 121, 180–197, 2016.

Jung, C., Tél, T., and Ziemniak, E.: Application of scattering chaos to particle transport in a hydrodynamical flow, Chaos, 3, 555–568, 1993.

Karrasch, D., Huhn, F., and Haller, G.: Automated detection of coherent Lagrangian vortices in two-dimensional unsteady flows, P Roy Soc A - Math Phy, 471, 20140 639, 2015.

Klingbeil, K., Mohammadi-Aragh, M., Gräwe, U., and Burchard, H.: Quantification of spurious dissipation and mixing - Discrete variance decay in a Finite-Volume framework, Ocean Model, 81, 49–64, 2014.

Koh, T. Y. and Legras, B.: Hyperbolic lines and the stratospheric polar vortex, Chaos, 12, 382–394, 2002.

Leprince, S., Barbot, S., Ayoub, F., and Avouac, J. P.: Automatic and precise orthorectification, coregistration, and subpixel correlation of satellite images, application to ground deformation measurements, IEEE T Geosci Remote, 45, 1529–1558, 2007.

Madrid, J. A. J. and Mancho, A. M.: Distinguished trajectories in time dependent vector fields, Chaos, 19, 013 111–1–18, 2009.

Mahoney, J., Bargteil, D., Kingsbury, M., Mitchell, K., and Solomon, T.: Invariant barriers to reactive front propagation in fluid flows, Europhys Lett, 98, 44 005, 2012.

Mahoney, J. R. and Mitchell, K. A.: Finite-time barriers to front propagation in two-dimensional fluid flows, Chaos, 25, 087 404–1–10, 2015.

Mancho, A., Small, D., and Wiggins, S.: A tutorial on dynamical systems concepts applied to Lagrangian transport in oceanic flows defined as finite time data sets: Theoretical and computational issues, Phy Rep, 437, 55–124, 2006.

Mancho, A., Wiggins, S., Curbelo, J., and Mendoza, C.: Lagrangian Descriptors: A method of revealing phase space structures of general time dependent dynamical systems, Commun Nonlinear Sci, 18, 3530–3557, 2013.

Martin, A.: Phytoplakton patchiness: the role of lateral stirring and mixing, Prog Oceanogr, 57, 125–174, 2003.

Martin, A., Richards, K., Bracco, A., and Provenzale, A.: Patchy productivity in the open ocean, Global Biogeochem Cy, 16, 9–1, 2002.

McIlhany, K. and Wiggins, S.: Eulerian indicators under continuously varying conditions, Phys Fluids, 24, 073 601, 2012.

McIlhany, K., Mott, D., Oran, E., and Wiggins, S.: Optimizing mixing in lid-driven flow designs through predictions from Eulerian indicators, Phys Fluids, 23, 082 005, 2011.

McIlhany, K., Guth, S., and Wiggins, S.: Lagrangian and Eulerian analysis of transport and mixing in the three dimensional, time dependent Hill's spherical vortex, Phys Fluids, 27, 063 603, 2015.

Mendoza, C. and Mancho, A.: Hidden geometry of ocean flows, Phys Rev Lett, 105, 038 501–1–4, 2010.

Mendoza, C. and Mancho, A.: Review Article: "The Lagrangian description of aperiodic flows: a case study of the Kuroshio Current", Nonlinear Proc Geoph, 19, 449–472, 2012.

Mendoza, C., Mancho, A., and Rio, M.-H.: The turnstile mechanism across the Kuroshio current: analysis of the dynamics in altimeter velocity fields, Nonlinear Proc Geoph, 17, 103–111, 2010.

Mezić, I., Loire, S., Fonoberov, V. A., and Hogan, P.: A New Mixing Diagnostic and Gulf Oil Spill Movement, Science, 330, 486–489, 2010.

Mitchell, K. A. and Mahoney, J. R.: Invariant manifolds and the geometry of front propagation in fluid flows, Chaos, 22, 037 104–1–13, 2012.

Morrow, R. and Le Traon, P.-Y.: Recent advances in observing mesoscale ocean dynamics with satellite altimetry, Adv Space Res, 50, 1062–1076, 2012.

Nencioli, F., Dong, C., Dickey, T., Washburn, L., and McWilliams, J. C.: A Vector Geometry-Based Eddy Detection Algorithm and Its Application to a High-Resolution Numerical Model Product and High-Frequency Radar Surface Velocities in the Southern California Bight, J Atmos Ocean Tech, 27, 564–579, 2010.

Okubo, A.: Horizontal dispersion of floatable particles in the vicinity of velocity singularities such as convergences, Deep Sea Research and Oceanographic Abstracts, 17, 445–454, 1970.

Olascoaga, M. J. and Haller, G.: Forecasting sudden changes in environmental pollution patterns, PNAS, 109, 4738–4743, 2012.

Onu, K., Huhn, F., and Haller, G.: LCS Tool: A Computational Platform for Lagrangian Coherent Structures, Journal of Computational Science, 7, 26–36, 2015.

Oschlies, A. and Garçon, V.: An eddy-permitting coupled physical-biological model of the North-Atlantic, sensitivity to advection numerics and mixed layer physics, Global Biogeochem Cy, 13, 135–160, 1999.

Petersen, M. R., Williams, S. J., Maltrud, M. E., Hecht, M. W., and Hamann, B.: A three-dimensional eddy census of a high-resolution global ocean simulation, J Geophys Res: Oceans, 118, 1759–1774, 2013.

Rossi, V., López, C., Sudre, J., Hernández-García, E., and Garçon, V.: Comparative study of mixing and biological activity of the Benguela and Canary upwelling systems, Geophys Res Lett, 35, 2008.

Sadarjoen, I. A. and Post, F. H.: Detection, quantification, and tracking of vortices using streamline geometry, Comput Graph, 24, 333–341, 2000.

Sandulescu, M., Hernández-García, E., López, C., and Feudel, U.: Kinematic studies of transport across an island wake, with application to Canary islands, Tellus A, 58, 605–615, 2006.

Sandulescu, M., López, C., Hernández-García, E., and Feudel, U.: Plankton blooms in vortices: the role of biological and hydrodynamic timescales, Nonlinear Proc Geoph, 14, 443–454, 2007.

Sturman, R. and Wiggins, S.: Eulerian indiators for predicting and optimazing mmixing quality, New J Phys, 11, 075 031, 2009.

Tang, W. and Luna, C.: Dependence of advection-diffusion-reaction on flow coherent structures, Phys Fluids, 25, 106 602–1–19, 2013.

Thacker, W. C., Lee, S.-K., and Halliwell, G. R.: Assimilating 20 years of Atlantic XBT data into HYCOM: a first look, Ocean Model, 7, 183–210, 2004.

Weiss, J.: The dynamics of enstrophy transfer in two-dimensional hydrodynamics, Physica D: Nonlinear Phenomena, 48, 273–294, 1991.

Wiggins, S.: The dynamical systems approach to Lagrangian transprt in oceanic flows, Annu Rev Fluid Mech, 37, 295–328, 2005.

Wiggins, S. and Mancho, A.: Barriers to transport in aperiodically time-dependent two-dimensional velocity fields: Nekhoroshev's theorem and "Nearly Invariant" tori, Nonlinear Proc Geoph, 21, 165–185, 2014.

Wilson, M. M., Peng, J., Dabiri, J. O., and Eldredge, J. D.: Lagrangian coherent structures in low Reynolds number swimming, J Phys-Condens Mat, 21, 204 105, 2009.

Wischgoll, T. and Scheuermann, G.: Detection and visualization of closed streamlines in planar flows, IEEE T Vis Compu Gr, 7, 165–172, 2001.

Yang, Q., Parvin, B., and Mariano, A.: Detection of vortices and saddle points in SST data, Geophys Res Lett, 28, 331–334, 2001.

Supplemental material of: Detecting and tracking eddies in oceanic flow fields: A ~~vorticity~~ Lagrangian descriptor based ~~Euler-Lagrangian method~~on the modulus of vorticity

Rahel Vortmeyer-Kley[1], Ulf Gräwe[2, 3], and Ulrike Feudel[1]

[1]Institute for Chemistry and Biology of the Marine Environment, Theoretical Physics/Complex Systems, Carl von Ossietzky University Oldenburg, Oldenburg, Germany
[2]Leibniz Institute for Baltic Sea Research, Rostock-Warnemünde, Germany
[3]Institute of Meteorology and Climatology, Leibniz University Hannover, Hannover, Germany

Correspondence to: Rahel Vortmeyer-Kley (rahel.vortmeyer-kley@uni-oldenburg.de)

S1 ~~Seeded eddy model~~

~~The model is inspired by the seeded eddy model of a turbulent flow described in Abraham (1998) and the model of Jung et al. (1993). The model consist of n eddies and a background flow u_0 in positive x-direction.The stream function for an eddy field with n eddies is given by~~

$$\psi(\boldsymbol{x},t) = \sum_{i=1}^{n} (-1)^{m_i} \cdot w_i \cdot \exp(-\kappa_i((x-x_i)^2 + \alpha(y-y_i)^2)) + u_0 \cdot x$$

~~where $\kappa_i^{-1/2}$ is linked to the radius of eddy i with vortex strength w_i. The eddy i emerges at position $(x_i\ y_i)$. The radii of the eddies are drawn from a distribution of 1000000 eddies possessing a power law $1/r^3$. The distribution is normalized and allows eddies between $R_{min} = 10$ km and $R_{max} = 50$ km. Because we are interested in mesoscale eddies (15-25 km radii) we first draw a sample of 100 radii from the distribution and then pick randomly 10 sample radii that are between 15 km and 25 km. The position of these eddies is drawn from an uniform distribution. Half of the eddies rotates counter-clockwise and the other half clockwise. The factor m_i decides if the eddy rotates clockwise or counter-clockwise. If m_i is even the eddy rotates clockwise if m_i is odd the eddy rotates counter-clockwise.The model is parametrized such that it yields a dimensionless model. Lengths are measured in units of the maximal eddy radius of the mesoscale eddies and time is in units of the lifetime of an eddy which is the same for all eddies. The parametrization is given in Table **??**. Dimensional and dimensionless parameters of the seeded eddy model Parameter r T_c α κ u_0 $w$dimensional 25 km 30 d 1 $1/r^2$ 0.18 ms^{-1} $55 \cdot 10^3 \mathrm{m}^2\mathrm{s}^{-1}$dimensionless 1 1 1 1 18.66 200~~

Table S1. Dimensional and dimensionless parameters of the hydrodynamical model of a vortex street

Parameter	r	T_c	α	κ	L	u_0	y_0	w
dimensional	25 km	30 d	1	$1/r^2$	150 km	0.18 ms^{-1}	12.5 km	~~$55 \cdot 10^3 \mathrm{m}^2\mathrm{s}^{-1}$~~ $55 \cdot 10^3\ \mathrm{m}^2\mathrm{s}^{-1}$
dimensionless	1	1	1	1	6	18.66	0.5	200

S2 The hydrodynamic model of a vortex street

The ~~hydrodynamical~~ hydrodynamic model of the vortex street is an adapted version of the model by Jung et al. (1993). ~~Jung et al. (1993) models~~ They model the flow in a channel behind a cylinder in ~~the middle of the channel~~ its middle (cf. Jung et al. (1993) and Sandulescu et al. (2006) for details).

Here this model is modified in such a way that two counter rotating eddies that develop at times t and $t + T_c/2$ at position $(1, y_0)$ and $(1, -y_0)$ respectively, travel a distance L in positive x-direction within their lifetime T_c and fade out. The model is artificial because the impact of the cylinder on the eddy formation and its shading are neglected here making the eddy formation non-physical out of ~~the blue~~nowhere. However, since all quantities to be estimated by the eddy tracking tool are then given analytically, ~~makes~~ this artificial model makes up an ideal test bed for numerics.

Hence, the model is simplified as follows:

$$\Psi(x, y, t) = -wh_1(t)g_1(x, y, t) + wh_2(t)g_2(x, y, t) + u_0 y. \tag{1}$$

The first two terms describe the life cycle of the eddies of opposite sense of rotation. The vortex strength is given by w. The dynamics of the eddy evolution is modelled as the modulation of the amplitudes by the function $h_1(t) = |\sin(\pi t/T_c)|$ resp. $h_2(t) = h_1(t - T_c/2)$. The function $g_i(x, y, t) = \exp(-\kappa_0((x - x_i(t))^2 + \alpha(y - y_i(t))^2))$ with $i = 1, 2$ models the Gaussian shaped effect of the eddies on the stream function. The movement of the eddy centres is expressed by $x_1(t) = 1 + L(t/T_c \mod 1)$, $x_2(t) = x_1(t - T_c/2)$ and $y_1(t) = y_0 = -y_2(t)$. ~~(In case of type 3 noise, the noise is added to the y_1 and y_2 terms.)~~ The factor $\kappa_0^{-1/2}$ is the radius and determined as a characteristic linear size of the eddies and α is the ratio between the elongations of the eddy in x and y direction. In our case α is set to 1 (circular eddies). The last term describes the background flow with the velocity u_0.

The parametrization of the flow is chosen as in Sandulescu et al. (2006). Lengths are measured in units of the eddy radius r and time in units of the lifetime T_c of an eddy. The dimensional and dimensionless parameters are given in Table S1. The vortex strength is furthermore varied to study its impact on the eddy evolution.

S2 Algorithm of the eddy tracking

The key ideas of the algorithm (eddy detection, eddy tracking and eddy shape) inspired by the eddy tracking package by Nencioli et al. (2010) are schematically presented in this section.

Fig. S1 presents the concept of eddy detection. Similar algorithms can be constructed for the modulus of the vorticity and for the Okubo-Weiss criterion (~~with respect to~~ taking into account the fact that eddy cores are minima in case of Okubo-Weiss).

Fig. S2 shows idea of the eddy tracking.

Fig. S3 presents the eddy shape detection based on the ~~combination of the Euler-Lagrangian~~ modulus of vorticity based Lagrangian descriptor M_V ~~and the Lagrangian descriptor M.~~ based on the modulus of vorticity. The eddy shape detection searches for the largest closed contourline with the largest gradient of M_V along the contour line. To maximise these two conditions at the same time, we maximise a quantity that combines this two ideas: (Area enclosed by the contour line)·((∑ gradient of M_V along contour line)/(length of contour line)). Because contour lines surround the eddy core like the layers of an onion, maximising the enclosed area includes maximising the length of the closed contourline. Maximising the gradient of M_V along the contourline is linked to the idea to search for a singular line (the eddy boundary).

In case of eddy shape detection for realistic oceanic velocity fields like the example of the western Baltic Sea, the coordinates of the eddy cores have to be understood as candidates for the eddy core.

From all candidates for eddy cores only those are kept which fulfil the following conditions:

- The convexity deficiency as defined in Haller et al. (2016) has to be smaller than a threshold.
- No land is enclosed in the contourline.
- The contourlines are longer than a threshold length. The reason for that criterion is mainly to speed up the computation. Very short contourlines can typically be found very close around the eddy cores. Therefore, they need not to be checked for the gradient of M_V, because they will not describe the eddy boundary.

This set of eddies can then be used as input for eddy tracking.

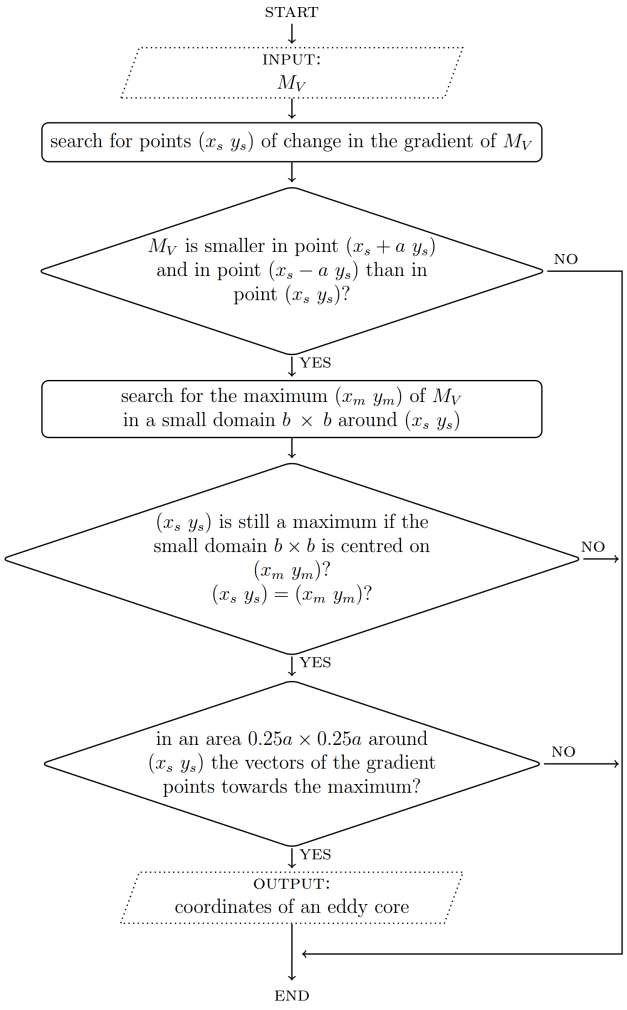

Figure S1. Schematic sketch of the eddy detection algorithm based on ~~Euler-Lagrangian~~ Lagrangian descriptor M_V.

References

Abraham, E. R.: The generation of plankton patchiness by turbulent stirring, Nature, 391, 577–580, 1998.

Haller, G., Hadjighasem, A., Farazmand, M., and Huhn, F.: Defining coherent vortices objectively from the vorticity, J Fluid Mech, 795, 136–173, 2016.

Jung, C., Tél, T., and Ziemniak, E.: Application of scattering chaos to particle transport in a hydrodynamical flow, Chaos, 3, 555–568, 1993.

Nencioli, F., Dong, C., Dickey, T., Washburn, L., and McWilliams, J. C.: A Vector Geometry-Based Eddy Detection Algorithm and Its Application to a High-Resolution Numerical Model Product and High-Frequency Radar Surface Velocities in the Southern California Bight, J Atmos Ocean Tech, 27, 564–579, 2010.

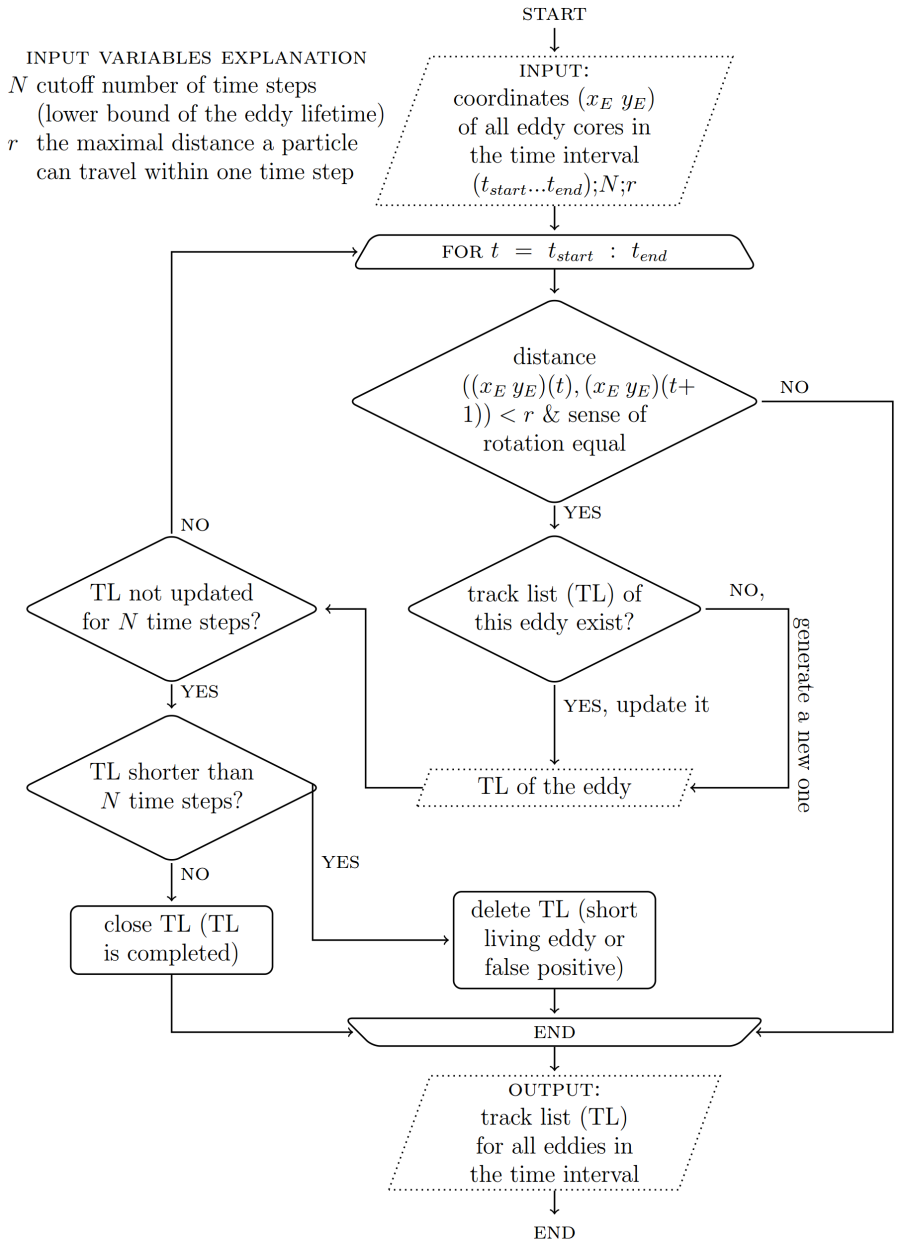

Figure S2. Schematic sketch of the eddy tracking algorithm based on ~~Euler-Lagrangian~~ Lagrangian descriptor M_V.

Sandulescu, M., Hernández-García, E., López, C., and Feudel, U.: Kinematic studies of transport across an island wake, with application to Canary islands, Tellus A, 58, 605–615, 2006.

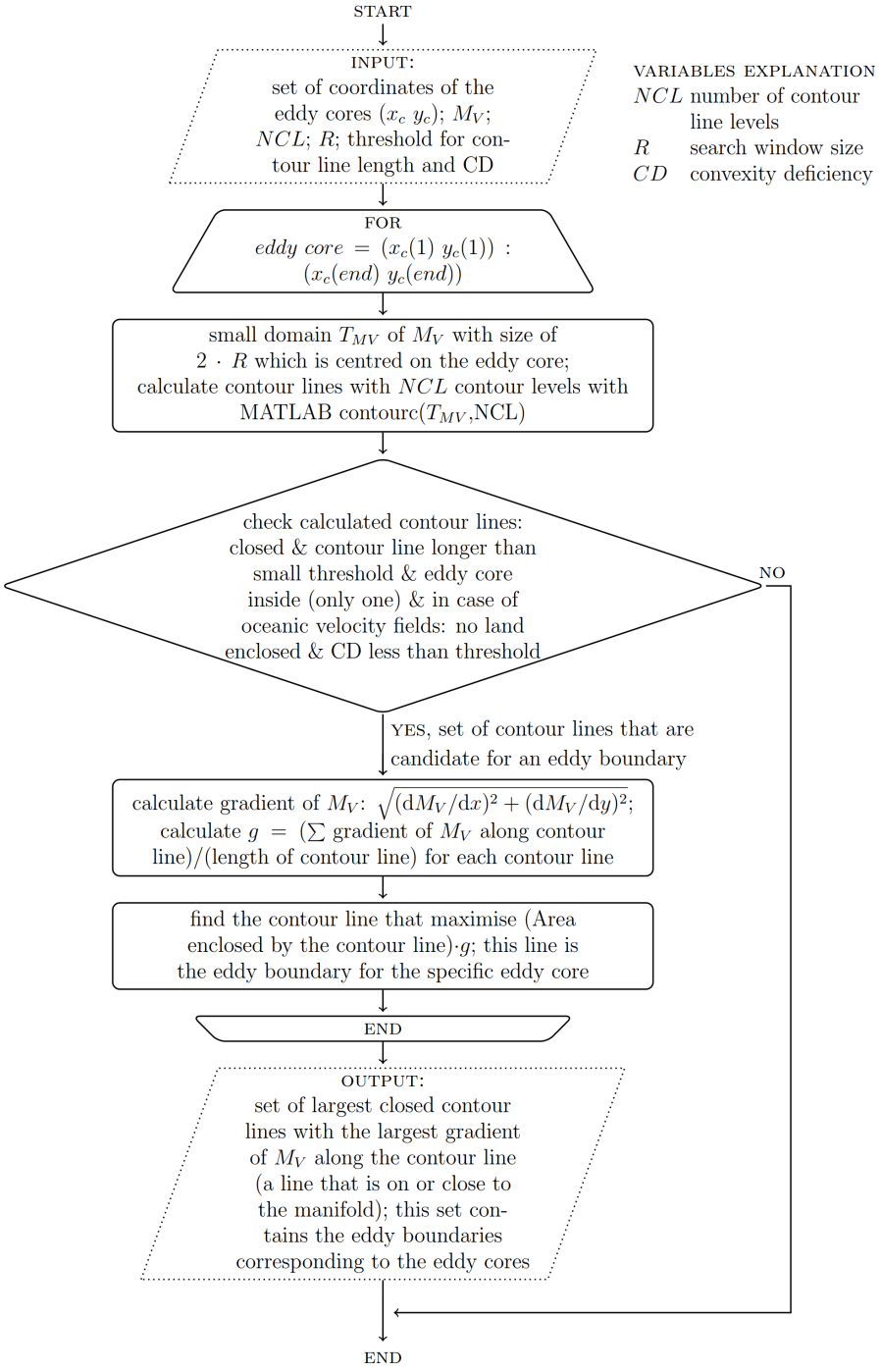

Figure S3. Schematic sketch of the eddy shape algorithm based on the ~~combination of the Euler-Lagrangian descriptor M_V and the~~ Lagrangian descriptor ~~M~~M_V.